

1-1-2023

Performance evaluation of single stand and hybrid solar water heaters: A comprehensive review

Zohreh Rahimi-Ahar

Mehdi Khiadani
Edith Cowan University

Leile Rahimi Ahar

Abdellah Shafieian
Edith Cowan University

Follow this and additional works at: <https://ro.ecu.edu.au/ecuworks2022-2026>



Part of the [Civil and Environmental Engineering Commons](#)

[10.1007/s10098-023-02556-6](https://doi.org/10.1007/s10098-023-02556-6)

Rahimi-Ahar, Z., Khiadani, M., Rahimi Ahar, L., & Shafieian, A. (2023). Performance evaluation of single stand and hybrid solar water heaters: A comprehensive review. *Clean Technologies and Environmental Policy*, 25(7), 2157-2184. <https://doi.org/10.1007/s10098-023-02556-6>

This Journal Article is posted at Research Online.
<https://ro.ecu.edu.au/ecuworks2022-2026/2570>



Performance evaluation of single stand and hybrid solar water heaters: a comprehensive review

Zohreh Rahimi-Ahar¹ · Mehdi Khiadani² · Leile Rahimi Ahar³ · Abdellah Shafieian²

Received: 13 February 2023 / Accepted: 28 May 2023
© The Author(s) 2023

Abstract

In this review, flat plate and concentrate-type solar collectors, integrated collector–storage systems, and solar water heaters combined with photovoltaic–thermal modules, solar-assisted heat pump solar water heaters, and solar water heaters using phase change materials are studied based on their thermal performance, cost, energy, and exergy efficiencies. The maximum water temperature and thermal efficiencies are enlisted to evaluate the thermal performance of the different solar water heaters. It is found that the solar water heaters' performance is considerably improved by boosting water flow rate and tilt angle, modification of the shape and number of collectors, using wavy diffuse and electrodeposited reflector coating, application of the corrugated absorber surface and coated absorber, use of turbulent enhancers, using thermal conductive working fluid and nanofluid, the inclusion of the water storage tank, and tank insulation. These items increase the heat transfer area and coefficient, thermal conductivity, the Reynolds and Nusselt numbers, heat transfer rate, and energy and exergy efficiencies. The evacuated tube heaters have a higher temperature compared to the collectors with a plane surface. Their thermal performance increases by using all-glass active circulation and heat pipe integration. The concentrative type of solar water heaters is superior to other solar heaters, particularly in achieving higher water temperatures. Their performance improves by using a rotating mirror concentrator. The integration of the system with energy storage components, phase change materials, or a heat pump provides a satisfactory performance over conventional solar water heaters.

✉ Mehdi Khiadani
m.khiadani@ecu.edu.au

Zohreh Rahimi-Ahar
z.rahimi@velayat.ac.ir

Leile Rahimi Ahar
L-rahimi-ahar@iau-ahar.ac.ir

Abdellah Shafieian
a.shafieianastjerdi@ecu.edu.au

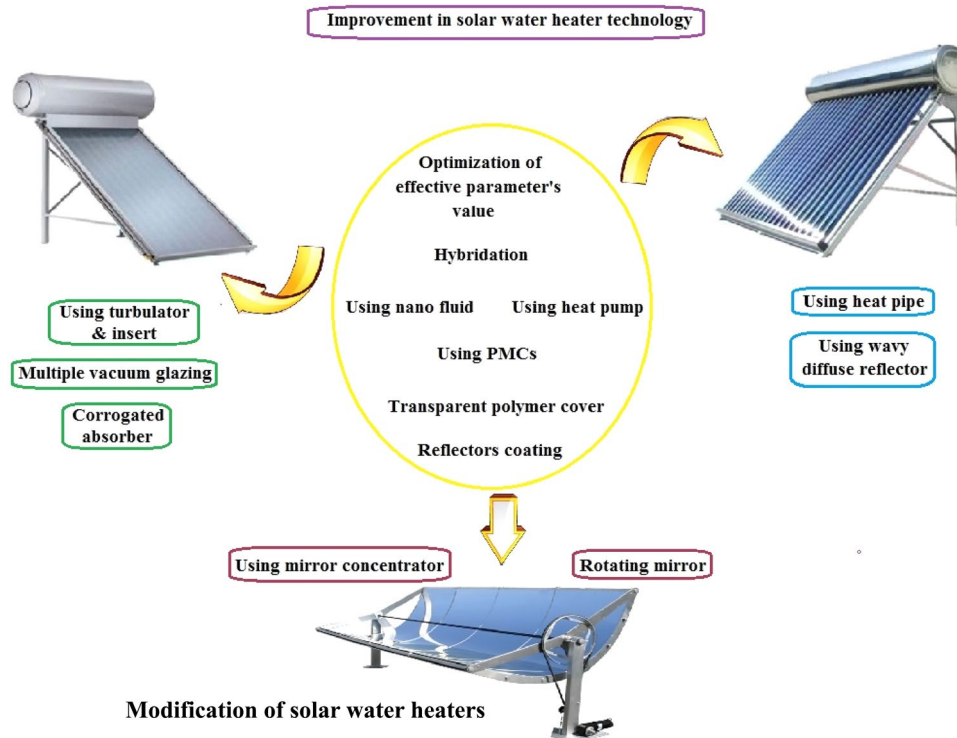
¹ Department of Chemical Engineering, Engineering Faculty, Velayat University, Iranshahr, Iran

² School of Engineering, Edith Cowan University, 270 Joondalup Drive, Joondalup, Perth, WA 6027, Australia

³ Department of Chemistry, Ahar Branch, Islamic Azad University, Ahar, Iran

Graphical abstract

Modification of solar water heaters



Keywords Solar energy · Solar water heaters · Energy storage · Phase change materials

Abbreviation

C	Collector
CFD	Computational fluid dynamics
COP	Coefficient of performance
CPC	Compound parabolic concentrator
CT	Coiled turbulator
CSC	Coconut shell charcoal
DWHR	Drain water heat recovery
DX-SAHP	Direct-expansion solar-assisted heat pump
EFDM	Explicit finite difference method
FPC	Flat plate collector
ETC	Evacuated tube collector
GRL-HPI	Gravity return loop heat pipe
HP	Heat pump
HPI-SC	Heat pipe solar collector
ICS	Integrated collector–storage system
MT	Matrix turbulator
PCM	Phase change material
PTC	Parabolic trough collector
PV/T	Photovoltaic/thermal
SA	Stearic acid
SWH	Solar water heater
TES	Thermal energy storage

T-SWH	Thermosyphon-based solar water heater
WG	Water-in-glass

Introduction

Energy is contextual for human activities. In the past, fossil fuels were used as the primary energy source; however, renewable energies are recently considered a game-changer for development (Strielkowski et al. 2021). Energy policies in some countries are aimed to provide sustainable and secure energy. To this end, renewable energies play a leading role (Siampour et al. 2021). A solar water heater (SWH) converts solar energy into heat and heats water flowing through it. Accordingly, the water temperature is increased for various applications. Financial estimations are a decision-making factor in using an SWH (Almutairi et al. 2021). Consumers require information about the cost and performance of different SWHs against electrical or fossil fuel-driven water heaters as a critical deciding factor for adopting SWHs in the future (Sharma 2021).

Studies on SWH usage in China, Turkey, Taiwan, Africa, Middle East countries, etc. have revealed some useful financial and environmental results, which will be covered in this

study. It is estimated that 610,500 kg of CO₂ per month can be saved by installing 10,330 SWHs in the towns, though hot water consumption may vary by household (Curry, et al. 2017). The policy measures implemented for the contribution of SWHs confirm reducing the 300–500 kg of CO₂ emission per year from the residential sector (Yamaguchi et al. 2013). Future research would explore the coevolution patterns of environmental and economic motivations by comparing the incentives provided by the government toward the innovations that lower carbon emissions in regions at a progressing stage (Yu and Huang 2020). Markets remain robust by lower payback periods and availability of local dealers/installers. With the government subsidy program and the implementation of tax breaks and tax credits, an SWH can be favorably compared to electrical or fossil fuel-running water heaters (Nasirov et al. 2021). The financial characteristics of the SWHs could give a life cycle saving of €4280.0 over a payback period of 5 years (Koroneos and Nanaki 2012). In Turkey, the SWHs decrease the annual greenhouse gas emissions by 790 kt CO₂-eq and save \$162.5 M/yr via the reduction in imports of natural gas (Uctug and Azapagic 2018). SWH use in Malaysia saves 2 billion kWh of electricity and prevents the emission of 1560 kt of CO₂ per year (Jing 2015).

SWHs are classified into direct and indirect circulation cycles. In the direct type, water is circulated through the system using a pump, while in the indirect circulation system, a non-freezing fluid is circulated through the collectors using a pump. The heat is transferred to the water using a heat exchanger (Peng et al. 2023). A schematic of these two types of SWHs is illustrated in Fig. 1.

A flat plate collector (FPC) was the first design of any SWHs before the introduction of concentrative collectors. The evacuated tube collector (ETC) containing heat pipe (HPI) and water-in-glass evacuated tube solar water heater (WGET-SWH) types has been proposed for evacuated tube-type solar water heaters (ET-SWHs) (Shafieian et al. 2019a, b). The integrated collector–storage (ICS) schemes have also been introduced. In conventional SWHs, the collection and storage are in separate units, and the water is circulated through the system either via a pump or by natural convection. In ICS-SWHs, the same configuration serves as the collector and storage system (Farzan et al. 2023).

Different designs of SWHs are presented in Fig. 2. In FPCs, an absorber tube with various configurations absorbs the solar energy and heats the water which moves in it. This tube is installed in a box with a glass top cover, insulated bottom, and walls. The ET-SWH has parallel rows of glass tubes. Each tube includes a glass outer tube and a metal or glass absorber tube. The inner tube absorbs solar energy, and the space between the inner and outer tubes is evacuated to prevent heat loss. It is categorized into all-glass passive circulate, all-glass active circulate, and heat pipe integrated

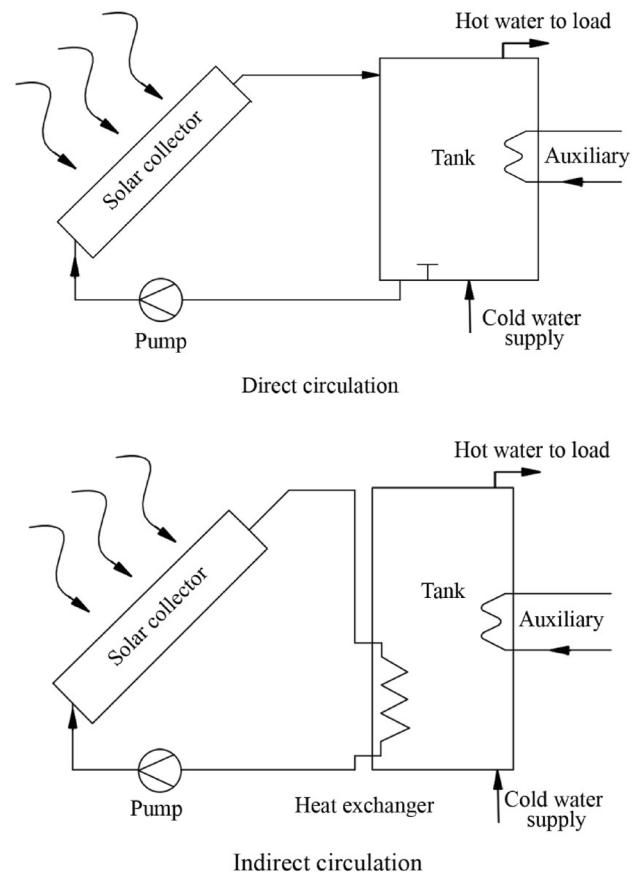


Fig. 1 Schematic of the direct and indirect SWHs

types. In the first category, natural convection causes water heating, and the heated water moves into the water storage tank. In the second category, the water moves down from the cold manifold, and after heating using solar energy, it moves up to the hot water manifold. In the third category, volatile fluid in a sealed component strengthens thermal energy absorption. The parabolic trough collector (PTC) uses the mirrored surface of a linear parabolic reflector to focus solar radiation onto an absorber pipe. Consequently, the hot water flows through the absorber pipe. The design of an SWH depends on the geographical location, weather and operating conditions, heat loss, human error, consistency and coherency of data, collector type, tilt angle, conductivity of the working fluid, etc. The energy and exergy efficiencies are used to characterize the thermal performances of SWHs (Shrivastava et al. 2017).

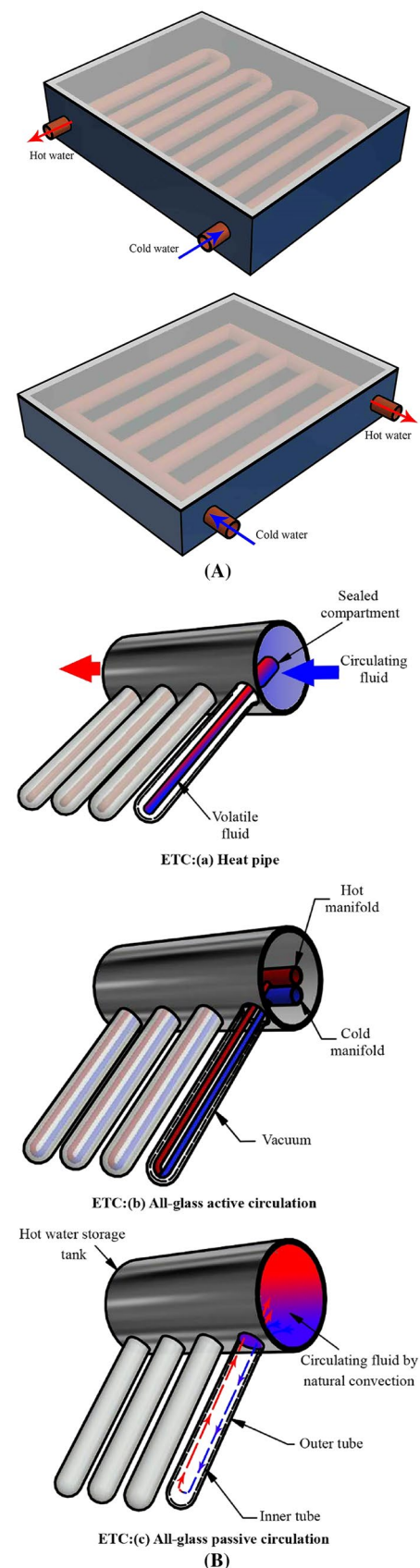
The collectors with thermosyphon flow are commonly used for domestic and small-capacity applications. Water flowing through the collector absorbs heat and flows naturally toward the storage tank. Water in the collector is replaced by cold water through a header at the bottom of the collector. A thermosyphon-based solar water heater (T-SWH) requires an uninterrupted supply of cold water.

Fig. 2 Type of solar collectors: **A** flat plate collector: serpentine and parallel tubing, **B** evacuated tube collector, **C** parabolic trough collector (Milani and Abbas 2016)

Forced flow SWHs are used where an uninterrupted supply of hot water is required all day and night. The water in the collector heats up as the collector is exposed to the sun. As the water temperature reaches the preset temperature, a control system switches ON the pump, and the water is forced into the water storage tank. The hot water in the collector is replaced with cold water. As the temperature decreases below the preset value, the pump is switched OFF. This cycle continues during the operation. The flow diagrams of the thermosyphon-based and forced-type solar collectors are presented in Fig. 3.

In ICS-SWH, the storage and auxiliary equipment are eliminated due to the esthetic view of their installation on the rooftop; hence, the cost is reduced. ICS-SWH contains a heater and an insulated tank. The qualitative behavior of any SWH is predicted through the solution of the main differential equations and the steady-state or transient conditions in much better quantitative agreement with the experiment. Operating at atmospheric pressure and a partial vacuum is noticeable. Utilizing a partial vacuum is tricky and may decrease the performance of the system, while the heat loss coefficient also reduces at vacuum (Farzan et al. 2023). The schematic of an ICS-SWH is presented in Fig. 4.

Unique features and advantages of SWHs have turned them into attractive options for solar applications and drawn significant attention in recent years. To date, several studies have been published summarizing findings relevant to the utilization of SWHs in various forms and configurations. However, to the authors' knowledge, a comprehensive review that surveys and provides an overview of the studies carried out to improve the thermal performance of solar water systems (mainly during the last decade) by implementing different strategies has not been published to date. Therefore, in this paper, the latest strategies, methods, and designs to enhance the performance of these systems along with their effectiveness, contribution, advantages, and disadvantages were reviewed and discussed. Flat plate- and concentrate-type solar collectors, ICS systems, SWHs combined with PV/T modules, solar-assisted heat pump SWHs, and SWHs using phase change material (PCM) were studied based on the thermal performance, cost, energy, and exergy efficiencies. Other review papers have concentrated on the thermal performance of either one type of SWH or the thermodynamic analysis, while this paper has focused on all related topics to SWHS to shade a way for future research. Moreover, challenges and research gaps were identified and recommendations for future research potentials were presented.



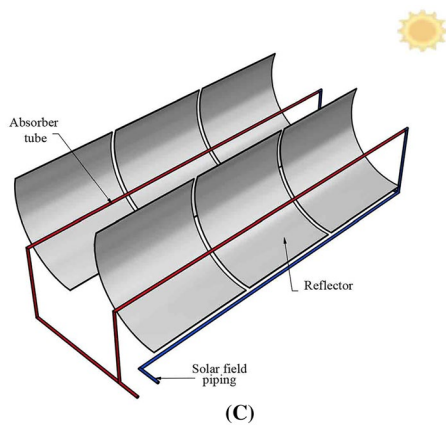


Fig. 2 (continued)

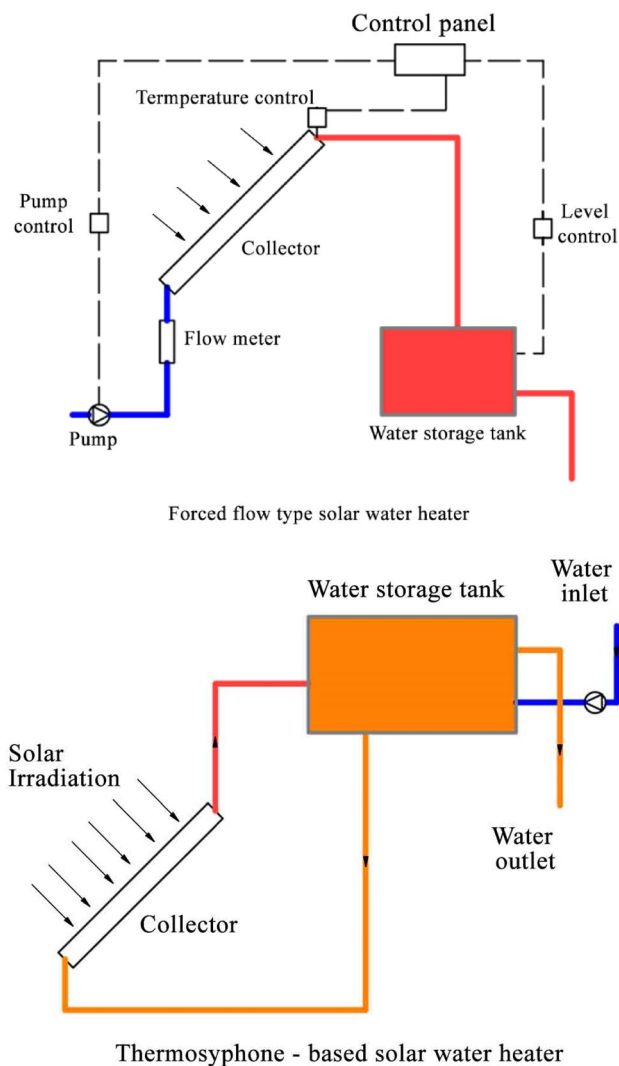


Fig. 3 Flow diagram of the forced-type and thermosyphon-based SWHs

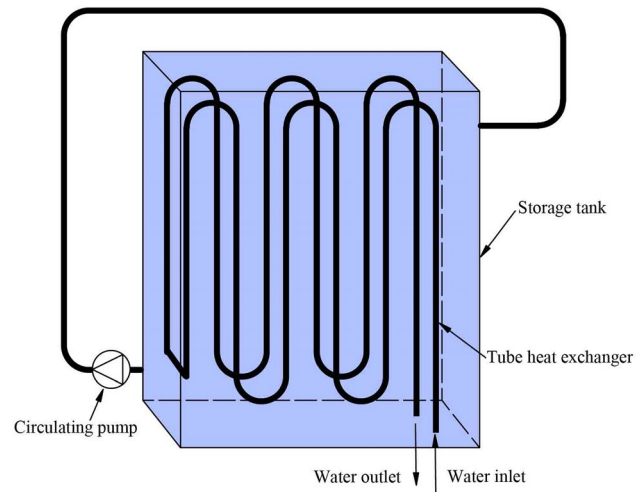


Fig. 4 Schematic of the ICS-SWH (Gertzos et al. 2008)

Design strategies

Flat plate- and concentrate-type solar collectors have been used to supply heat to SWHs. Their performance is compared using outlet water temperature from a collector or storage tank, as well as energy and exergy efficiencies, and overall cost. It has been proved that the concentrative collectors with sufficient area and time let the water be adequately heated. Moreover, HPI, PCM, heat pump (HP), and reflector integration can boost the performance of an SWH. In the following sections, the thermal performance of the flat plate solar water heaters (FP-SWH), cylindrical solar water heaters (C-SWH), parabolic trough solar water heaters (PT-SWH), hybrid solar water heaters (H-SWH) and SWHs incorporating PCMs will be reviewed.

Flat plate solar water heaters (FP-SWH)

FP-SWHs are categorized based on their absorber characteristics, flow inserts, vortex generators, and insulation material. Conventional and once-through designs have been developed. Water is continually cycled through the panels in the conventional design, while in the once-through type, the water passes once through the solar panel and then enters the hot water storage tank (Karwa et al. 2018). It has been tried to enhance the heat transfer coefficient, decrease the pressure drop and heat loss, and overcome the drawback of the conventional SWHs by saving solar energy for the early morning, late evening, and nighttime applications (Venkatesan and Senthil 2020). The double-glassed FP-SWH performs better than the single-glassed type due to a lower heat loss to the atmosphere (Nirmala 2020). The schematic of the double-glassed and single-glassed FPCs is presented in Fig. 5.

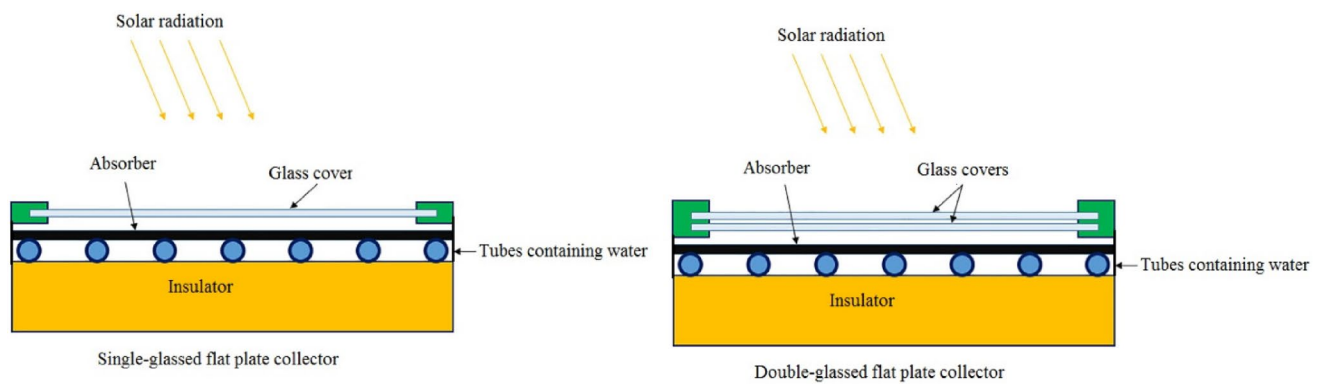


Fig. 5 Schematic of the single- and double-glazing flat plate collectors

The performance study of the FP-SWH with three types of twisted tape experimented by Almeshaal et al. (2020) confirmed the positive effect of using twisted tape inside the riser tubes as a turbulator. The geometric profile of a riser tube in an FP-SWH was modified by creating the dimples inside the riser tube (Arun et al. 2020). It caused turbulence and swirl flow throughout the riser to improve the heat transfer. The experimental and computational fluid dynamics (CFD) results were compared. The hot water output increased at the low water flow rates, while at higher flow rates, it was moderately constant. Twist ratio variation from 3 to 12 led to heat transfer rate improvement by 18–70%, though the pressure drop augmented by about 87–132%, as compared to a plane collector. Due to the lower plate temperature, the heat loss decreased (Kumar and Prasad 2000). The thermal efficiency of an FP-SWH with pebble stones as a porous medium and the riser tube containing an agitator was developed by Kanimozhi et al. (2019). Placing an agitator and the pebble stones increased the convective heat transfer and reduced thermal loss leading to a slow increase in energy efficiency. The maximum energy efficiency of 86.4% and 59.59% was obtained in the case of SWH without and with an agitator, respectively. Using a hindrance promoter was another option to improve the thermal performance of an FP-SWH (Rohit Khargotra and Kumar 2021). At the optimal values of the parameters, the hindrance promoter improved the Nusselt number by 4.56 times higher than the smooth tube. The rectangular-winglet- and delta-winglet-type vortex generators within the circular tube of an FPC were simulated (Da Silva 2019). The vortex generators were coupled to augment the heat transfer rate between tube walls and working fluid. The primary and corner vortices were recognized on the flow, which increased the heat transfer rate, even though the corner vortex was more obvious for the rectangular-winglet generator (independent of the attack angle and Reynolds number). The secondary flow produced by the inserts through the corner vortex was observed via the rectangular-winglet generator. A maximum heat transfer

rate resulted in 45° for vortex generators. However, the optimum ratio between the rate of heat transfer and the drop in pressure penalty was obtained at 30° for the delta-winglet generator. Modifications of the risers are illustrated in Fig. 6.

The absorber is the heart of an SWH, which absorbs the sunlight and warms up the water. The efficiency of a collector depends on the absorptance and emittance of the absorber. There is an urgent need to develop highly efficient, structurally, thermally, optically, and mechanically stable solar absorber coating. The emittance is comparatively less significant than the solar absorptance. Most solar collectors use spectrally selective absorber coating with low emittance and high absorptance at the infrared spectrum and in the solar range, respectively (Bello and Shanmugan 2020). The collector with the electrodeposited coating had a better performance than the one coated with CuO. At temperatures $>50^\circ\text{C}$, it performed similarly to a TiO_2 -based collector. This was due to lower heat losses from the backside of the Cu flat plates with a Ni coating (Lizama-Tzec et al. 2019). Coating the absorber with black chrome and nickel–cobalt coating on copper and using the reflectors improved the heat absorption. The system's thermal efficiency with a nickel–cobalt absorber was higher due to its higher emittance than the black chrome panel. By increasing the flow rate, more heat was absorbed leading to higher thermal efficiency while a further increase in flow rate decreased the time of heat absorption and led to a lower thermal efficiency (Ramesh et al. 2022). Furthermore, free convection took place inside FPCs with boosted flow rates. Hence, the water flow rate should be boosted according to the solar radiation intensity, collector area, and temperature difference between the hot water leaving the collector and the cold water entering it. The maximum outlet temperature of about 96°C was obtained as the CuO/ H_2O mixture absorbed more heat due to more heat transfer coefficient at high temperatures. Due to the short contact time of the nanoparticle inside the riser tubes, a lower water temperature was obtained in forced circulation. The copper, copper oxide, aluminum oxide, and

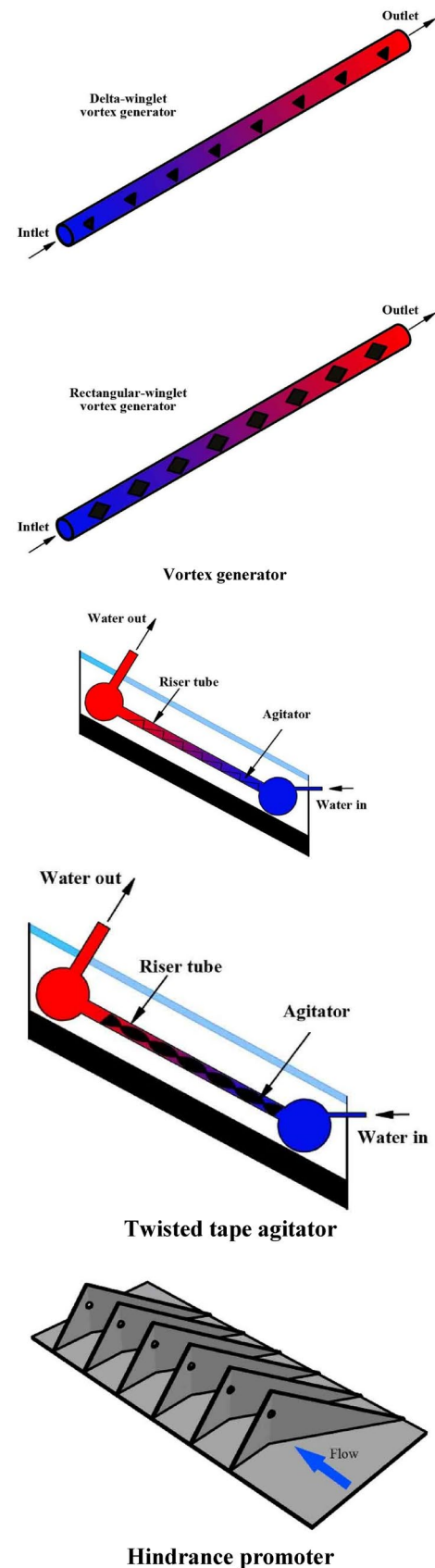
Fig. 6 Schemes of the vortex generator (Almeshaal et al., 2020), ► twisted tape agitator (Kumar and Prasad 2000), and hindrance promoter (Rohit Khargotra and Kumar 2021)

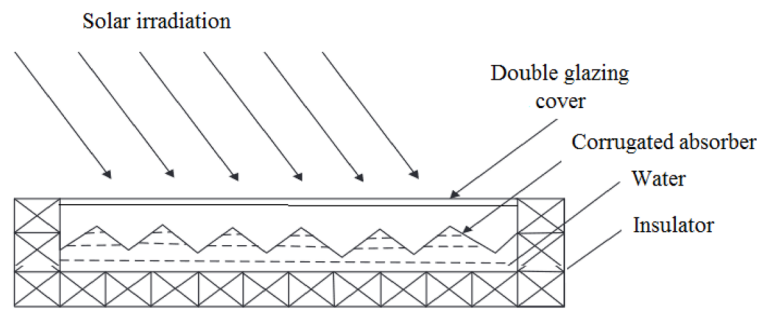
titanium oxide nanoparticles in water were used to improve the thermal performance of an FP-T-SWH (Darbari and Rashidi 2021). Among the introduced nanoparticles, copper oxide had the best thermal efficiency. The useful energy and energy efficiency increased by increasing the flow rate (higher Reynolds number and the heat removal factor, leading to an improvement in the convective heat transfer rate inside the tubes and a reduction in the thermal resistance between the fluid inside the absorber and the tube) and volume fraction of nanoparticles (due to a reduction in the average temperature of the absorber, hence, a lower heat loss). The maximum energy efficiency of 80% was obtained at a solid volume fraction of 0.05 for the solar intensity of 200 W/m^2 . The ambient temperature variation from 20 to 40°C enhanced the energy efficiency by 5.5%, while, when the water temperature increased from 30 to 55°C , it reduced the energy efficiency by 15%. Using a mixture of CuO–MgO (0.1–0.1%) in an FP-SWH also showed better performance compared to pure water (Janardhana et al. 2022).

In SWH containing corrugated-surface-based absorber without flow rate, the highest water temperature reached 58°C and 78°C during winter and spring, respectively. In the case of the absorber with flow rate, the daily energy efficiency of the solar collector increased from 59 to 67%, when the mass flow rate increased from 0.005 to 0.013 kg/s (Yassen et al. 2019). A comparative analysis of the performance of circular and a trapezoidal surface with absorber tubes indicated better performance of the trapezoidal surface over the circular absorber by energy and exergy efficiency improvement by about 4% and 6%, respectively, due to the reduction in the heat loss (Sharma, 2022). The sinusoidally folded absorber sheet also ensured a higher water temperature, hence a higher flow rate compared to a flat plate absorber. It means the collector's useful gain is linked with the flow rate and by increasing the gain, the flow rate also increases via the collector (Yehualashet et al. 2022). Different types of absorber plates are presented in Fig. 7.

The effect of the tracking orientations such as vertical-axis (V), north–south (NS), east–west (EW), and inclined east–west (IEW) on SWH's performance was numerically investigated. The Perez diffuse model with the hourly weather data was utilized. The study provided a comprehensive outlook to adopt the FPC incorporated with various single-axis and dual-axis trackers in the northern hemisphere (Bahrami et al. 2022). The collector installation at an improper angle reduced the received solar radiation.

An ICS-SWH is a water heating system that alchemizes solar radiation directly into heat (Rao and Somwanshi 2022). The highest collection efficiency can be increased





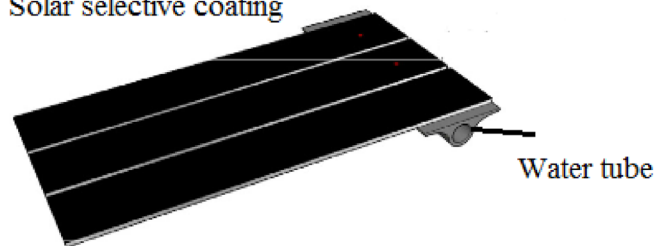
(a) Corrugated type absorber (Mokhlif et al., 2021)

Cross section photo of the micro heat pipe array



Micro heat pipe array

Solar selective coating



(b) Micro heat pipe array absorber (Deng et al., 2015)

Fig. 7 Schematic of the different absorbers. **a** Corrugated-type absorber (Mokhlif et al. 2021), **b** micro-heat pipe array absorber (Deng and Yu 2016)

by 36.17%. Despite many advantages of these systems, high heat losses during the night decreased the efficiency of the system. Introducing baffle plate structure, insulation of tank, connecting tanks in series, using PCMs and reverse thermosyphon valve minimized the heat losses from the system.

Cylindrical solar water heaters (C-SWH)

Designing a C-SWH with a high heat collection rate is complex. Many investigations have been performed to improve its design and thermal performance. High-throughput screening (HTS) technique using machine learning estimates the probable combinations of extrinsic properties of these heaters. ET-SWHs have the disadvantages of slow water temperature increase as well as a slow response to loading, which can be rectified using an optimum closed-loop pulsating HPI (Siritan et al. 2022). The solar radiation intensity is the main parameter affecting the SWH performance. At higher solar radiation intensity, water viscosity decreases, and the density gradient becomes more significant for similar temperature differences, leading to a more significant driving force and producing natural circulation. The ET-SWH containing argon in the space between the cover and

the absorber is also recommended due to the lower Prandtl number of argon in comparison with the air (Sadeghi et al. 2019).

In SWH with a low tilt angle, the cold water of the storage tank moves down along the lower wall of tubes and then returns to the storage tank along the upper wall of tubes, whereas, for the SWH with a high tilt angle, the situation in the morning is the same as the SWH with a low tilt angle (Fig. 2B). In the afternoon, the cold water from the storage tank moves down (fully or partially mixed with the hot water) and then returns to the water storage tank. The shorter tube distance leads to worse thermal performance due to more sun shading between tubes.

The performance of T-ET-SWH and ET-SWH incorporating 20 wickless HPIs containing methanol was compared. The inner glass tube was coated with Al–N/Al. Daily efficiency improvement of the system by HPI over the thermosyphon system was 22.5%, 32.4%, and 42.5% for no loading, continuous loading, and intermittent loading, respectively (Al-Joboory 2019). The T-ETC modeling showed the explicit finite difference method (EFDM) makes a better accuracy than the thermal resistance technique (Wannagosit et al. 2018). The effect of working fluid (e.g., ammonia,

methanol, acetone, pentane, and water) on the technical performance of an ET-SWH investigated by Arab and Abbas (2013) resulted in the superiority of the ammonia against its counterpart owing to a sudden decrease in the thermal resistance between 9 and 15 h.

The performance of two designs of a WGET-SWH (220-L tank and 2.9 m² collector area; in-tank boost: Design A and preheater with boost tank: Design B) was compared with an FPC (300-L tank and 3.7 m² collector area) by TRNSYS (Budihardjo and Morrison, 2009). The thermal performance of two FPCs was better than that of a WGET-SWH. The performance of ETC was less sensitive to tank size. Annual energy savings of FPC, Design A, and Design B were 77%, 70.9%, and 66.2%, respectively. Coupling a larger tank with Design B resulted in a minor reduction in annual solar fraction, representing the improved collector performance. Two ET-SWHs with the same area were modeled. One utilized internal HPI condensers (Case 1), whereas the other used external ones (Case 2) (Redpath 2012). Case 1 was 17% more efficient than Case 2. These systems were feasible for hot water production in northern maritime climates.

The thermal performance of an ET-SWH at six ETC tilt angles (15°, 20°, 25°, 30°, 35°, and 40°) was evaluated (Kumar et al. 2023). The highest thermal efficiency was 75.04% at the tilt angle of 15°, which was 5.3%, 11.6%, 12.8%, 17.5%, and 18% more than the efficiency at tilt angles of 20°, 25°, 30°, 35°, and 40°, respectively. The lowest energy payback time was 1.14 years at this tilt angle. The payback time was from 1.67 to 2.26 years at other tilt angles. The energy payback time was minimum for ETC installed at a tilt angle of 15°. WGET-SWH produced high levels of stratification at low tilt angles ($\beta < 27^\circ$), which was comparable to those obtained in systems with stratification baffles or promoters (Bracamonte 2017). This result was confirmed by an 18% higher thermal efficiency at a tilt angle of 15° compared to a tilt angle of 40°. Using a shorter tube was recommended due to better thermal performance than a longer one and less probable to be damaged during transportation. It was found that compact concrete absorbers in SWH with a spiral tube arrangement are more cost-effective than traditional flat plate collectors. In this arrangement at the lowest mass flow rate (0.005 kg/s) inside the spiral tube, the maximum water temperature in typical sand and concrete absorbers reached 75 °C and 70 °C, respectively (Edwin et al. 2023).

A major disadvantage of the ETCs is the weak circulation of water at their lower end. It makes them inactive most of the time and decreases the effective absorber area. Using turbulators and the flat and wavy diffuse reflectors can overcome this disadvantage. The incorporation of turbulators significantly improves the performance of the ET-SWH by introducing turbulent flow within the tubes. The investigations presented that the water temperature in the

tank reached 75 °C, 79 °C, and 81 °C for plain (without twisted tapes) ETC, ETC equipped with flat and wavy diffuse reflectors, respectively. The wavy diffuse reflector had better performance due to the extra energy saving in the range of 12.2–16.7% at different zones. An optimized ETC consisting of 10 tubes with a reflector showed the importance of the distance between tubes as well as the distance between the reflector and collector (Arun et al. 2020; Kong et al. 2020a, b, c). Experiments on ETC with matrix turbulator (MT-ETC), ETC with coiled turbulator (CT-ETC), and ETC without turbulator (simple ETC) revealed that the turbulator-equipped designs could significantly enhance the tube mean temperature (Vasanthaseelan et al. 2021). The plain ET-SWH, ET-SWH with a twist ratio of 2 (Twist 2), and the ET-SWH with a twist ratio of 3 (Twist 3) were experimented with by Gunasekaran et al. (2021). The inserts reduced velocity and provided a uniform temperature distribution. They augmented the heat transfer at moderately high temperatures. The inserts avoided conducive heat transfer at a low temperature. The daily thermal efficiency of the plain ET-SWH, Twists 2 and 3 were 68.4%, 75.2%, and 73%, respectively. The photograph of CT, MT, and twisted tape designs is shown in Fig. 8.

Parabolic trough solar water heaters (PT-SWH)

FPCs and ETCs are widely used for water heating systems; however, incorporating other types of more efficient solar collectors based on the concentration concept in water heating applications can enhance energy savings and environmental impacts. CPCs are one of the promising solar collectors for domestic hot water applications. The concentrating collectors are equipped with mirrored surfaces to concentrate the solar energy on its receiver which is positioned at the focal point of the surface. Water flows into the receiver and absorbs the heat. These collectors reach much more temperatures than FPCs and ETCs. A good concentrator should be designed to improve the energy efficiency of the SWHs. Performance comparison of the empty tube PTC and PTC-equipped rings attached to different twisted tapes presented that the attachment of the ring improves the heat transfer rate; however, it augments the pressure drop. To overcome the pressure drop, modification should be made in the rings. It has been concluded that the Nusselt number increases up to 101% for the modified rings leading to a thermal performance improvement of 24% (Isravel et al. 2020). The feasibility of utilization of CPC in several locations worldwide (latitudes of 0, 15, 30, 45, and 60°N) by solar radiation range of 2509–852 kWh/m² and electricity cost range of 0.04–0.28 USD/kWh was investigated. In locations with high electricity costs, even in cases of low solar radiation, investment in CPC had the highest profits (Gilani and Hoseinzadeh, 2021). Preheating of boiler feed water

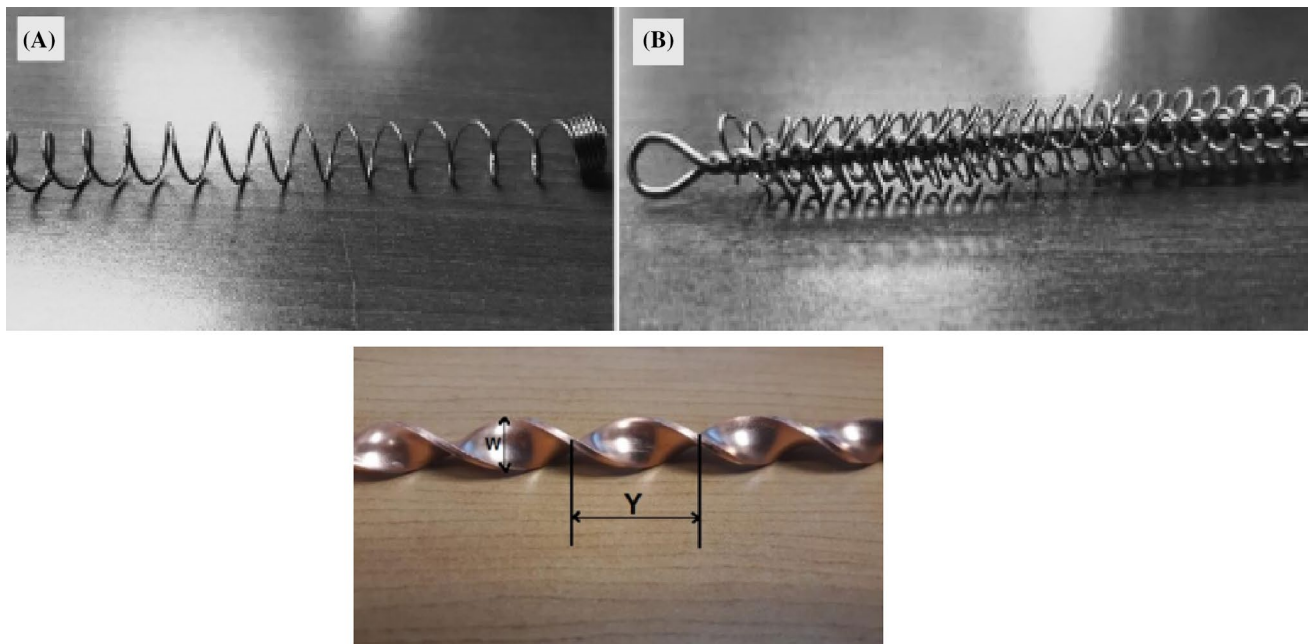


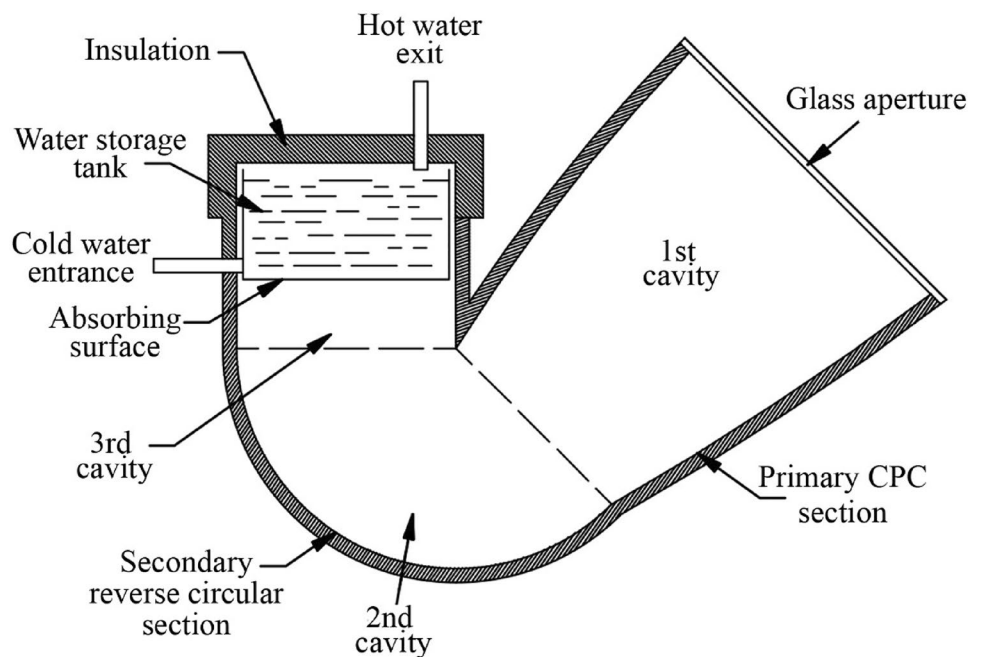
Fig. 8 Photograph of **a** coiled turbulator, **b** matrix turbulator (Vasanthaseelan et al. 2021), twisted tape (Gunasekaran et al. 2021)

(Pathak et al. 2021), generating steam for use in the textile industries (Eskin 2000), water treatment (Li et al. 2022), and desalination plants (Rahimi-Ahar and Hatamipour 2020) are the applications of CPC technology. CPC by providing hot water of $> 60\text{ }^{\circ}\text{C}$ can also be used in medium-sized food industries (Ktistis et al. 2021; Yılmaz et al. 2023).

ICS-SWHs convert solar radiation into heat at a considerable conversion rate. It consists of the main components

of a vessel and a reflector. Figure 9 presents the schematic of an ICS-PT-SWH. Due to the inherent freeze protection of an ICS-SWH, it offers a promising technique for water heating in colder climates. These compact systems are of low cost with a high solar collection efficiency. The thermal analysis on an ICS-CPC showed that mirror, steel sheet, and aluminum foil have the maximum daily efficiencies of 66.7%, 47.6%, and 43.7%, respectively (Panahi et al. 2019).

Fig. 9 Schematic of ICS-SWH (Smyth et al. 2005)



Selecting a proper concentrator, controlling hot water withdrawal, coupling the absorber to the storage tank, and developing an ICS-SWH system increase the thermal efficiency of SWHs. The position of the absorber pipe relative to the PTC substantially affected the system's efficiency by 70% while for an absorber pipe positioned at the focal line of the collectors, it was less than 60%. An increase in the solar radiation intensity decreased the thermal efficiency of the proposed systems. The lowest and the highest efficiencies were in July and April, respectively. It means the highest efficiency was obtained on colder days or in colder areas (Avargani et al. 2020).

The thermal performance of SWH was evaluated for transparent baffles positioned at various parts in the collector cavity. The baffles positioned at the upper part of the exit aperture of the CPC decreased the thermal losses by convection suppression without a meaningful increase in the optical losses (Smyth, et al. 2005). The CPC using a plastic substrate permitted the heater to reach an optical efficiency of nearly 65%. The energy efficiency of 55–35% was obtained in the proposed design depending on the solar radiation intensity (Smyth et al. 2004). An ICS-SWH equipped with a linear PTC with a reflector made of rectangular and rotating mirrors was designed by Harmim et al. (2019). The setup was effective during winter with a daily efficiency of 36.4–51.6%. Under a clear sky with an initial water temperature of 22 °C, the water temperature reached 49 °C. The schematic of an ICS-SWH containing a PTC with rotating mirrors is shown in Fig. 10.

An ICS-SWH was theoretically studied to evaluate the thermal and optical behaviors of the heater and clarify the effect of the truncation. The heater consisted of the upper part with two parabolic sections and the lower part with three involute reflectors. The concentration ratio and the height of the upper concentrating stage were important parameters. A maximum temperature of about 60 °C was obtained for full and truncated CPC. For the full CPC, the direct solar ray falling on the aperture plane provided more reflections before reaching the absorber, while for truncated CPC, less reflection was made. It means a reduction in the mean number of reflections had a positive influence on the optical performance of the studied heater. A reduction in the size of the storage tank was suggested to maintain an acceptable level of the mean temperature (Benrejeb et al. 2016). The reflection of the solar radiation on the CPC reflectors was simulated using a ray-tracing model in an ICS-SWH consisting of two symmetrical parabolic and three involute reflectors (Kong et al. 2020a, b, c). The design of the lower stage concentrator showed a meaningful enhancement in optical efficiency. The proposed system reached the maximum water temperature of 65 °C. The reflector shape was modified, in which the old reflector had three parabolic sections, and the modified one had two involute parts and two

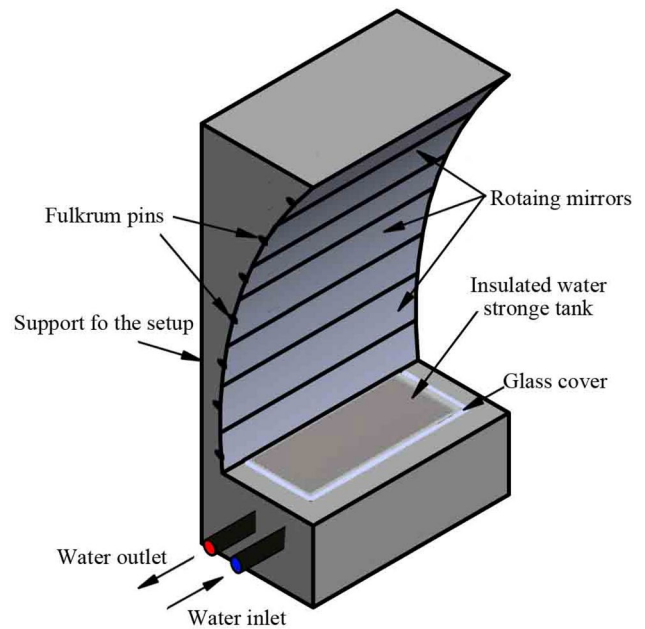


Fig. 10 Schematic of ICS-SWH containing a parabolic reflector with rotating mirrors (Harmim et al. 2019)

parabolic sections; hence, the system size was reduced while keeping an acceptable level of the mean water temperature. This truncation reduced the manufacturing cost and facilitated its installation.

Hybrid solar water heaters (H-SWH)

An FPC was equipped with a controllable sun tracker PV unit to increase the absorbed solar radiation. The heater produced hot water of 50 °C and electricity for the households in winter. The maximum overall average energy efficiency was 62% (Touaba et al. 2020). When the economic, environmental, and energy benefits were considered, the solar thermal system was more favorable compared with PV and PV/T systems. An ICS-SWH combined with a PV/T module offered a promising approach for water heating and electricity generation. A high tank water mass and the solar cell packing factor led to a high PV/T efficiency. It was due to the high temperatures of the solar cell and the water in the tank. The planar and tubular thermoelectric generators also could increase the quantity of the produced hot water (Fad-douli et al. 2020).

A direct-expansion solar-assisted heat pump water heater (DX-SAHP-WH) comprised of the electronic expansion valve, compressor, solar collector/evaporator, and condenser enhances the thermal performance of the heater by hybridization technology. Remote buildings in cold areas benefit from the winter heating system of air source HP coupled with an ET-SWH (Li et al. 2023).

The schematic of a typical DX-SAHP-WH is presented in Fig. 11.

A quasi-dynamic mathematical model of a DX-SAHP-WH was developed at different compressor speeds. The mathematical equations governing lumped elements were established to model the compressor and expansion valve. The uniform flow distributed parameter methods were used to model the unglazed FPC/evaporator and condenser. A minor impact of the compressor speed on the average coefficient of performance (COP) was noticed. Under distinctive working conditions, the COP reached above 4.6 for various compressor speeds, when the water temperature changed from 28.2 to 61 °C. When the mean compressor speed was reduced from 2910 to 2650 rpm, the COP increased by 7.5%. By increasing the compressor speed, the evaporating temperature stabilized while slowing down the compressor speed stabilized the compressor power (Kong et al. 2020a, b, c).

The multi-criteria optimization of a DX-SAHP-WH using R-134a by genetic algorithm (GA) was performed by the trial and error technique (Cao et al. 2020). The comparison of single- and bi-criteria optimization results confirmed the superiority of this optimization method. The bi-criteria optimization results revealed that collector efficiency was reduced by 1.6% compared to the primary model, while the COP improved by about 20%. The performance of the optimized heater was enhanced so that the working hours of the heater decreased to 109 h. In a DX-SAHP-WH, as the gas cooler outlet pressure and temperature increased, the water inlet temperature also increased; hence, the COP decreased. The relative humidity variation from 31.6% to 55.8% and solar radiation intensity increase from 30.17 to 876.9 W m⁻² increased the COP by 6% and 30%, respectively. The increase in solar radiation led to an increase in compressor suction and discharge temperatures, evaporating pressure, and water flow rate, while the reduction in the collector efficiency was concluded (Duarte et al. 2021). A DX-SAHP-WH comprised an expansion valve, a compressor, a micro-channel solar collector/evaporator, and a condenser was designed (Kong et al. 2020a, b, c). R290 with a refrigerant charge of

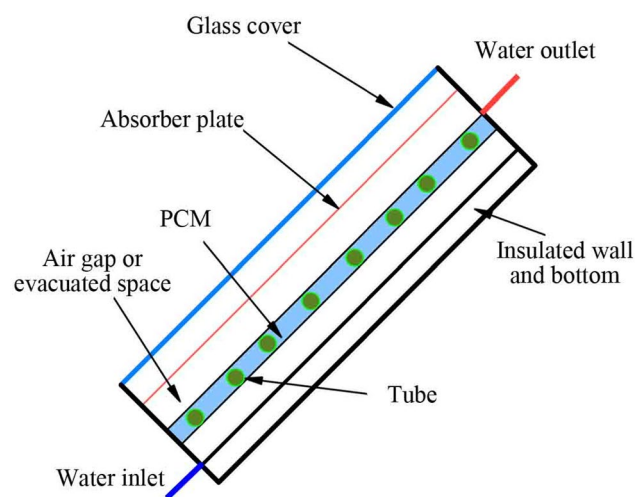


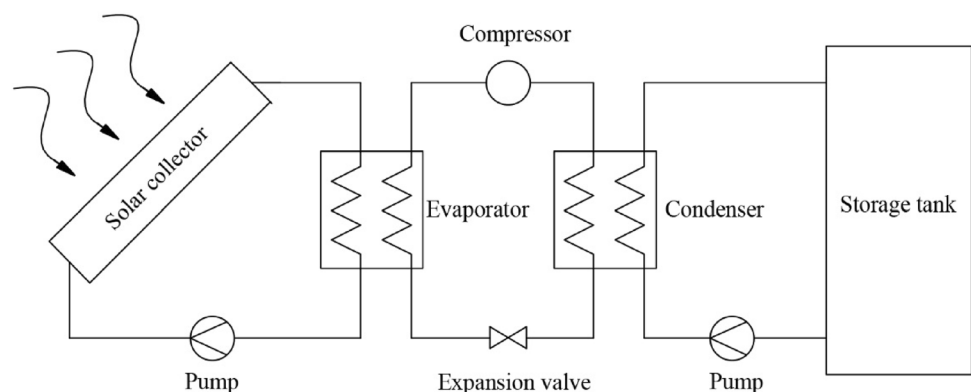
Fig. 12 Schematic of a solar water heater containing phase change material (Mandal et al. 2019)

410 g or 350 g were used, and the average COP ranged from 2.12 to 4.43. A DX-SAHP-WH charged with 800 g R134a produced water with a maximum temperature ranging from 55 to 60 °C, while the COP of the system was more than 3.0 (Kong et al. 2018). By increasing the ambient temperature or solar radiation intensity, the COP increased, while the heating time decreased. Modeling of DX-SAHP-WH, including the collector/evaporator under typical frosting conditions, presented the superiority in delaying frosting compared to the traditional evaporator (Kong et al. 2020a, b, c). The collector efficiency enhanced effectually during the growth of frost crystals.

Solar water heaters incorporating phase change material (PCM)

SWHs incorporating PCMs as thermal energy storage (TES) have been developed since the 1970s (Shalaby et al. 2020). A schematic of SWH containing PCM is illustrated in Fig. 12.

Fig. 11 Schematic of the DX-SAHP-WH (Nuntaphan et al. 2009)



PCMs are classified as inorganic, organic, and eutectic materials. They are encapsulated within the side surface of the storage tank. The remaining energy of PCMs helps in any sudden thermal loads during the night. PCMs categorize into solid–gas, solid–liquid, liquid–gas, and solid–solid states (Kee et al. 2018). The solid–liquid PCMs are commonly used in SWHs due to the limitations of the three other types of PCMs. The solid–solid types have relatively low heat transformation, significant volume variation, and high pressure in the existence of gas. During the daytime, the temperature of PCM increases, and PCM absorbs heat; it reaches the melting point and absorbs heat at a certain temperature. The PCM absorbs thermal energy and stores heat without a significant increase in temperature until all PCM melts. During the night, the surrounding temperature of the liquid PCM decreases and solidifies the material, consequently releasing the stored latent heat to the surrounding environment. Adding high thermal conductive fillers to a pure PCM improves thermal conductivity and stability, hence speeding up the heat storing and releasing rates during phase change. Forming a stable composite by polymerization, physical blending, or encapsulation is recommended. Notably, during the melting, the PCM is confined in the layered and the movement of the PCM is limited; hence, using stable composite PCM is strengthened. The integration of PCM increases the outlet temperature and extends the operating hours due to a thermal lag caused by energy storage, hence a delay in the temperature response (Tamuli and Nath 2023).

A proper PCM has a demanded melting/freezing temperature within the desired usage temperature range, high values of latent heat of fusion, thermal conductivity, specific heat, and density, a small difference between densities of solid and liquid phases, congruent melting of the materials, insignificant supercooling, high chemical stability, non-corrosivity, non-poisonous, nonflammability, non-explosivity, and abundant supply at a low cost (Liu et al. 2012). Adding nanofillers in lower concentration improves these characteristics and provides more hot water for the next day morning as compared to a conventional SWH. Several attempts have been made to increase the heat exchange between the water and PCM. Different PCMs used in SWHs, their characteristics, and their effect on the thermal efficiency of the SWH are tabulated in Table 1. Aluminum oxide nanofillers could augment the energy storing capacity of an SWH (Dhinakaran et al. 2020). PCM-containing nanofillers absorbed more heat energy and released the heat for a longer time, leading to a 33% increase in water temperature. The low thermal conductivity of the PCM was compensated by dividing the storage system into thin slices (Shalaby et al. 2020). Shell and finned tube latent heat storage system integrated with the FP-SWH design provided a large heat transfer area between the storage material and the working fluid. The maximum energy

efficiency of 65% was achieved when a paraffin wax/water mixture was used. This heater was able to provide hot water at a maximum temperature of 60 °C. A double-walled tank by embedding the PCM in the outer part of the tank with two positive functionalities of thermal insulation and thermal storage led to the highest water temperature of 80.3 °C and the maximum thermal efficiency of 74% at a water flow rate of 1.75 l/min. Moreover, the maximum thermal stratification occurred at a water flow rate of 1.25 l/min, and it weakened by increasing the flow rate (Yari et al. 2023). The thermal efficiency in an ET-SWH in stagnation mode (without water flow) was improved from 66 to 82% using PCM. By flowing mode variation from 10 to 27 l/h, no considerable reduction in the heat gain of the collector was observed; however, 40 l/h plunged the discharge efficiency (Sadeghi et al. 2022).

A mixture of paraffin wax and nano-CuO was used as a thermal energy reservoir (Mandal et al. 2019). An increase in the nano-CuO concentration in the CuO-PCM mixture decreased the outlet temperature of the water. This was because of the large volume/surface area of nano-CuO leading to transferring the maximum thermal energy to the water instead of absorbing it as well as the low heat capacity of CuO-PCM nanocomposite over the paraffin. A maximum temperature of about 58 °C was stored by base paraffin in the gap of 2 cm between the glazing and the absorber. It was concluded that the nano-CuO was not effective during the night. A solar storage tank coupled to a PCM (NaOAc, 3H₂O) module was simulated and showed that increasing the PCM amount reduced the melting and enhanced the heat losses to the surrounding (Bouhal et al. 2018). A PCM was prepared by modification of coconut shell charcoal (CSC) by H₂O₂ and then was stabilized by stearic acid (SA) (Xie et al. 2020). The thermal conductivity of the SA/CSC was about 2.9 times more than that of pure SA. The modified CSC appeared more super macropores contributed to the impregnation of SA than non-modified CSC. SA/CSC composite had excellent thermal stability at high working temperatures (180 °C). The composite was stable during phase change and had good thermophysical properties as well as more heat transfer efficiency than pure SA. The maximum temperature of the water leaving the FPC, CPC, and ETC was about 115, 105, and 104 °C, respectively.

The performance of ET-SWH was studied without PCM and using the paraffin and nano-CeO₂ diffused in paraffin with mass fractions of 0.5%, 1.0%, and 2.0%. PCM-containing nanoparticles was well performed because of the nonlinear increase in thermal conductivity by increasing the nanoparticle concentration. The PCM-containing 1.0% of nanoparticles used in thermosyphon-based WGET-SWH led to the maximum first and second law efficiencies of 89.15% and 8.59%, respectively (Kumar and Mysamy 2020). It was due to a low reduction in latent heat and proper shrinking of the gap between solidification and melting points. A set

Table 1 PCMs used in SWHs and their characteristics

PCM/nanoadditives	Latent heat of fusion (kJ/kg)	Melting point (°C)	Thermal conductivity (W/m.K)	Density (kg/m ³)	Specific heat (kJ/kg.K)	Energy efficiency (%)	Ref.
NA	189	49	NA	NA	NA	48	(Al Imam et al. 2023)
Paraffin	166.7	60.5	NA	NA	0.172	38.3	(Manirathnam et al. 2021)
SCi-CuO (1%)/paraffin	160.3	59.6	NA	NA	0.226	41.7	
Paraffin	140.2	63.74	0.18	NA	NA	69.64	(Kumar and Mylsamy 2020)
CeO ₂ (0.5%)/paraffin	137.8	63.44	1.255			76.11	
CeO ₂ (1%)/paraffin	135.7	62.66	0.313			79.2	
CeO ₂ (2%)/paraffin	108.6	63.01	0.376			76.77	
Paraffin wax (liquid)	189	53–74	0.17–0.47	822–1330	2.34–2.76	47–58	(Bazri et al. 2019)
Paraffin wax (solid)			0.22–0.57	917–1470	2.05–2.48		
NaOAc, 3H ₂ O	173	NA	5	1340	Liquid: 3.68 Solid: 4.02	NA	(Bouhal et al. 2018)
N-eicosane	237.4	36.5	Liquid: 0.16 Solid: 0.212	Liquid: 780 Solid: 820	Liquid: 2.2 Solid: 1.9	NA	(Allouhi et al. 2018)
Dual PCM tritriacotane/	256	72	NA	Liquid: 782 Solid: 810	Liquid: 1.11 Solid: 0.87	52.21	(Papadimitratos et al. 2016)
Erythritol	339.8	118	NA	Liquid: 1300 Solid: 1480	Liquid: 2.76 Solid: 1.38		
RT42 graphite	139.7	43	5	789	1.57	35	(Chaabane et al. 2014)
Myristic acid	189	54	Liquid: 0.19 Solid: 0.17	1000	3.67	40	
Cu(1%)/paraffin	160.3	60.5	0.226	976.5	Liquid: 2.1 Solid: 1.85	52	(Al-Kayiem and Lin 2014)
Paraffin	166.7	59.6	0.172	908.6	Liquid: 2.2 Solid: 1.905	51.1	
Stearic acid	186.5	60–61	0.18	Liquid: 1150 Solid: 1080	Liquid: 2.38 Solid: 2.83	50.3	(Sari and Kaygusuz 2001)

of ET-HP arrays coupled to a tank filled with three types of PCM based on paraffin wax was modeled (Bazri et al. 2019). The maximum energy efficiency of the PCM coupled with SWH on a sunny day was 54%, while this efficiency increased to 58% on a cloudy or rainy day. The average efficiencies of the heater containing three used PCMs were increased from 10 to 58% compared with the design without PCM.

A transparent glass cover was placed at 0.02 m from the absorber, polyurethane insulation, and using a copper pipe as a heat exchanger provided hot water of 75 °C. Paraffin wax, a paraffin wax nanocomposite with 1.0 wt% SCi and CuO, used as the PCMs in an ET-T-SWH (Manirathnam et al. 2021). The thermal conductivity of paraffin wax by the diffusion of CuO and SCi nanoparticles was meaningfully augmented (22.53%). The water temperature in the cases of PCM and nanocomposite PCM was 53 °C and 56 °C, respectively, while for the heater without PCM, it was 45 °C. The energy efficiencies were found to be approximately 34%, 38%, and 42%,

respectively, for ET-T-SWH without PCM, with PCM, and with nanocomposite PCM (Mandal et al. 2020). A double-pipe helical coil heat exchanger containing PCM (RT-50) in the annulus SWHs (creating a turbulent mode of water flow in the inner pipe) was simulated. The k-ε RNG turbulence model well described the turbulent flow. Among helical pitch, outer and inner pipe diameters, Reynolds number, and fluid inlet temperature, the outer and inner pipe diameters and fluid inlet temperature were the main factors influencing the storage system's design. The 1.5% and 42% increases in the inlet temperature and the inner pipe diameter enhanced the melting rate by 27% and 92%, respectively, while a 20% increase in the outer pipe diameter led to a 52% reduction in the melting rate (Najafabadi et al. 2022). Adding PCM into a mantled hot water tank increased the outlet water temperature in the tank compared to without a PCM case. Furthermore, placing the mantle resulted in rapid maximization of temperature within the tank. In addition, replacing the PCM tubes on the top section of the tank resulted in an enhancement of

19.6% in the outlet water temperature compared to the case without PCM (İzgi and Arslan 2022).

Solar water heater's performance

Some of the noticeable research along with key features and findings are listed in Table 2. The results can be summarized as follows:

- In FP-SWH, forced flow circulation and using a V-cut tube insert were the best options due to the water temperature and energy efficiency of 90 °C and 82%, respectively. The collector installation at a 10° tilt angle improved the water temperature and energy efficiency by 8 °C and 13%, compared to a collector installed at 30°. Using nanofluid increased the water temperature while having an insignificant effect on energy efficiency. A double-pass design can be a good candidate due to a low solar collecting area (0.135 m²) and high energy efficiency (77%).
- In cylindrical-type SWHs, the collector installation at a proper tilt angle and providing vacuum space between the absorber and outer glass cover had a significant effect on water temperature.
- SWH equipped with CPC with inserting nail-type twisted tape and stainless steel absorber had better thermal performance compared to the system containing aluminum and copper absorbers.
- In similar operating conditions and collector areas, the CPC-type collectors had the highest water temperature compared to the ETC and FPC types. Operation on cloudy days, rainy days, or dusty glass weakened the thermal performance of all types of solar heaters; hence, using PCM, TES, an insulated hot water storage tank, and cleaning the glass improved the thermal performance.

Thermodynamics and thermoeconomic studies

Several theories were introduced for the exergy analysis of a domestic SWH to save the cost and preserve its thermal efficiency in desired values (Rahimi-Ahar et al. 2020). The exergy losses from the storage tank and the collector due to imperfect thermal insulation should be considered. The exergy destruction via the collector and storage tank was caused by the irreversibility of heat transfer via the collector and irreversibility due to the mixing of water at various temperatures within the tank (Rahimi-Ahar and Hatami-pour 2023). The exergo-economic analysis of different

SWHs using conversion, utilization, and recycling procedures showed that the highest exergy efficiencies of the SWH by solar collecting areas of 2 m² and 4 m² were in the range of 2–3%. An increase in collector area decreased the exergy efficiency and increased the cost rate of irreversibility. Though the large collectors could collect further heat from the sun and had more input exergy, the output exergy from the collector was also high. The maximum exergy was destructed in colder seasons of the year due to the low exergy contents for output and input streams (Thangavelu et al. 2021). Using nanofluid in FP-SWHs could augment the exergy and energy efficiencies of the collector by up to 30% and 24%, respectively (Vengadesan and Senthil 2020). Up to a 30 °C increase in the outlet temperature of the water can be achieved using the Al₂O₃ nanoparticles compared to an SWH containing pure water (Sivasubramanian et al. 2022). An absorber plate coated with copper oxide nanoparticles (CuO NPs) increased the energy efficiency by about 36% compared to the exergy efficiency of SWH with flat absorber plates. The exergy efficiency improvement by this coating was about 11% higher than that of the matte black absorber (Nazari et al. 2022).

The solar PV/T system was introduced as an economic technology. The maximum energy and exergy efficiencies of 92.7% and 15.58% were obtained for an HPI-SWH by the optimum number of glass tubes during cold days (Shafieian et al. 2019a, b). The overall efficiency of an HPI-SWH was determined using an adjustable flow rate method regulating the working fluid mass flow rate by variation of the solar intensity. The plant operated in similar weather conditions using distilled water (Case I), the optimized nanofluid (Case II) at a constant flow rate, and the optimized nanofluid at a variable flow rate (Case III). The exergy efficiency of Cases II and III, respectively, increased by 1.58% and 2.66% more than that in Case I (Shafieian et al. 2019a, b). The thermodynamics analysis of a PCM layer coupled to the HPIs of an FPC was performed to evaluate the SWH performance during discharging and charging. For a higher PCM thickness, the latent heat storage improved the heating necessities at night and reduced the exergy efficiency. By increasing the PCM thickness, the difference between the melting and solidification times was increased, and the exergy was destroyed through heat transfer between the absorber and PCM. The energy and exergy efficiencies of 76.95% and 2.625% resulted in a system with PCM and 77.61% and 3.34% for a system without PCM, respectively (Hamed et al. 2017). It should be noted that the overall exergy and energy efficiencies are affected by water withdrawal flow rates and ambient temperature. The highest energy efficiency of a T-SWH reached 32% and 26% in summer and winter, respectively (Chargui, 2021).

A temperature-controlled SWH (TC-SWH) was exergetically studied at the temperature range of 40–55 °C and

Table 2 Thermal performance of SWHs

System	Collector type	Collector area (m ²)	Storage tank capacity (L)	Energy efficiency (%)	Max. water temperature (°C)	Main observations	Ref.
Compact SWH	FPC	0.67	138	82.88	90	The forced flow operation increased the efficiency	(Taheri et al. 2013)
Closed T-SWH	FPC	2.06	160	80	85	Increasing the ratio of temperature to incident radiation reduced the instantaneous efficiency	(Taherian et al. 2011)
V-trough SWH fitted with:	FPC	1	100	71.11	–	Twist 3 provided better performance compared to the plain tube and other twist ratios	(Saravanan et al. 2016)
				81.55		Helix had a higher Nusselt number than the helix with V-cut, and the V-cut had a higher Nusselt number than square cut	
				85		Correlation for calculation of the friction factor was developed	
				82.67		The size reduction of the solar collector was proposed	
PV panel combined with the wickless heat pipe SWH	FPC	1.875	–	70	72	Decreasing the collector area increased the thermal efficiency while reducing the water temperature within the tank	(Ziapour et al., 2016)
T-SWH	FPC	2.16	–	56.43	68.62	TS-SWH was economically competitive to the electric heaters, especially in a high electricity price and utilization factor	(Sae-Jung et al. 2015)
ICS-SWH with a baffle plate-type storage tank	FPC	–	110	65	74	The payback period was 5.4 years	(Ziapour and Aghamiri 2014)
						The storage tank divided by two trapezoids cross-sectional volumes had higher energy efficiency than a triangular water storage tank	

Table 2 (continued)

System	Collector type	Collector area (m ²)	Storage tank capacity (L)	Energy efficiency (%)	Max. water temperature (°C)	Main observations	Ref.
ICS-SWH	FPC	–	–	–	63	N-eicosane was used as the PCM	(Allouhi et al. 2018)
					64	Increasing the thickness of the PCM layer increased the cost because of the surplus mass of PCM consumed	
SWH using tube with	FPC	0.2709	10	55	56	Solar radiation had a significant effect on the melting/solidification	(Ram kumar et al., 2020)
				58	67	The nanofluids experienced no penalty of pump power	
						An increase in Reynolds number and volume fraction of the working fluid improved the convective heat transfer coefficients	
Double-pass SWH with rectangle conduits	FPC	0.135	–	77	–	The collector efficiency was enhanced by increasing the flow conduit aspect ratio, recycle ratio, and water flow rate nevertheless, it decreased by increasing the inlet water temperature	(Ho et al. 2010)
SWH with extra-long pulsating heat pipes	FPC	–	200	53.79	49.6	The used heat pipe with a filling ratio of 70% had the most stable condition, the highest heat transfer rate, and the most prolonged functioning duration	(Arab et al. 2012)
SWH with aluminum collector	FPC	3.61	302.8	80	63.3	The proposed collector improved the thermal efficiency by 12% over a conventional FPC during a day	(Robles et al. 2014)

Table 2 (continued)

System	Collector type	Collector area (m ²)	Storage tank capacity (L)	Energy efficiency (%)	Max. water temperature (°C)	Main observations	Ref.
SWH	FPC	1.3	100	60	60	The screen insulation during the night and mixing improved the collector performance	(Dharuman et al., 2006)
T-SWH with internal exchanger	FPC	2	95	50	58	The water temperature within the heat exchanger, the withdrawal water temperature, water flow rate, and the collector efficiency had a similar variation trend as the solar intensity and heat flux changes	(Koffi et al. 2014.)
				68.33	88		
V-through SWH	FPC	1	–	43	69	The tilt angle change from 15° to 25° increased the mean thermal efficiency from 27 to 30%	(Pandya and Behura 2017)
				46	60	The energy efficiency of clear glass and dusty glass was, respectively	
				48	55	Myristic acid as PCM stabilized the temperature and decreased the water tank volume and reserved the water temperatures at 51–52 °C during the night	
				49	50		
				–	–		
SWH	FPC	0.5	100	–	52		(Tarhan et al. 2006)
				–	39		

Table 2 (continued)

System	Collector type	Collector area (m ²)	Storage tank capacity (L)	Energy efficiency (%)	Max. water temperature (°C)	Main observations	Ref.
Conical-type SWH	With vacuum glass	2.3	200	72	–	The highest energy efficiency was achieved at a critical flow rate	(Hussain, and Lee 2014)
	Without vacuum glass			60			
SWH-PCM	ETC	1.272	–	58.55	–	PCM was Ba(OH) ₂ ·H ₂ O and BaCO ₃ The thermal performance of the proposed SWH was lower than WGET-SWHs The system was more efficient at a constant flow rate than under the condition of exposure By increasing the proportion of diffuse to radiation, the performance deteriorated	(Xue 2016)
Copper coil through SWH	ETC	0.112	–	41.2	66.2	A maximum temperature difference was created between the outlet and inlet of the coil at a water flow rate of 9 kg/h	(Al-Madani 2006)
SWH with inserting nail-type twisted tape	CPC	2.036	28	64.28	77.17	A lower twist ratio led to a higher hourly energy efficiency	(Bhakta et al. 2018)
ICS-SWH	Aluminum absorber	–	16.7	47.4	–	The sunlight was uniformly distributed around the absorber vessel	(Muhumuza et al. 2019)
	Copper absorber		16.7	51.6			
	Stainless steel absorber		27.7	48			

Table 2 (continued)

System	Collector type	Collector area (m ²)	Storage tank capacity (L)	Energy efficiency (%)	Max. water temperature (°C)	Main observations	Ref.
SWH in conjunction with a gas boiler drain water heat recovery (DWHR)	FPC	2.33	300	39.5	–	DWHR unit had a heat recovery of 789 kWh/year and overall effectiveness of nearly 50%	(Tanha et al. 2015)
	ETC	2.11		20.7	–	The efficiency decreased by increasing the temperature difference because of a lower solar intensity or a decline in the ambient temperatures The ETC had an unsatisfactory performance during winter in comparison with the FPC due to damaged tubes and the cover of tubes by ice or snow	
Conventional SWH	FPC	2.3	–	–	75	The solar fraction was 69%, 70%, and 80%, for FPC, CPC, and ETC, respectively, saving nearly 43 kWh/year, 13 kWh/year, and 29 kWh/year	(Bouhal, 2017)
	ETC	2	–	–	80		
	CPC	2	–	–	80		
All-glass SWH	ETC	0.564	40	–	67	The tilt angle had little effect on the thermal efficiency due to a low heat loss through the tubes, higher thermal stratification along the inactive area of the water storage tank	(Bracamonte et al., 2015)
					48	The water of the storage tank at the 45° tilt angle was thoroughly mixed at the end of the warming up	

compared with a T-SWH. The maximum energy efficiencies of 65% and 60% were obtained for the TC-SWH and T-SWH, respectively, due to the higher exergy content of hot water in the tank of TC-SWH (Ceylan 2012). A solar-assisted vapor injection HP cycle with a sub-cooler was developed to enhance the thermal performance of the traditional sub-cooler vapor injection HP cycle. An FPC of 5 m² was used, and energy and exergy efficiencies of 76% and 45% resulted. The energy efficiency of the cycle was enhanced with increasing solar radiation intensity, whereas the change in exergy efficiency showed an opposing tendency (Chen and Yu 2018).

Economic views

The levelized cost of heat includes capital costs, operating and maintenance costs, and all costs during its life. Each SWH should be modified to reduce the levelized cost. The SWHs address the economic potential in electricity saving, reducing CO₂ emission, and developing the related businesses and SWH industrial clusters (Mamouri and Bénard 2018). The techno-economical modeling of an HP-SWH by multi-energy cooperative utilization assisted in its commercialization. A government subsidy requires and the project has benefits for all investors who are involved (Li et al. 2019). The ET-SWH for Michigan's climate had a payback period as low as eight years (Mamouri and Bénard 2018). The cost of an SWH containing a linear Fresnel reflector was \$378.87, which could be recovered after 16 years from its first use (Said et al. 2021).

The techno-economic benefits of FP-SWHs using stainless steel, copper, and glass-lined storage tanks were evaluated through the Monte Carlo analysis. The SWHs with electric boosters and glass-lined storage tanks showed excellent thermal performance. The SWHs offered better long-term economic viability compared to the conventional systems at modest auxiliary energy consumption (Rezvani et al. 2017). The thermoeconomically optimization of an FP-SWH showed that mass flow rate and insulator thickness were the main deciding factors. At the same time, collector length did not affect the performance. For energy inputs of 0.5 kW, 1.5 kW, and 2 kW, the efficiency was enhanced by 0.123%, 0.740%, and 1.506%, compared to the energy input of 1 kW. The minimum annual saving of \$155.1 was obtained (Hajabdollahi and Hajabdollahi 2017). Long-term research led to lowering the cost of FP-SWH by replacing Cu tubes with Cu–Al plates and galvanized steel (G.S.)–Al tubes. A similar thermal performance was found by SWHs with Cu–Cu, Cu–Al, and G.S.–Al fins in FPC. The SWHs provided 100 L of water at an average temperature of 62 °C when the inlet water temperature to the heater was 23.9 °C. The cost of the SWH with Cu–Cu and G.S.–Al collectors

was \$136.7 (Rs. 10,250) and \$106.7 (Rs. 8000), respectively. The payback period varied between 2.92 and 4.53 years depending on the used fuel (electricity, firewood, or fossil fuels) (Nahar 2002). Economical comparison of the single-phase open T-ET-SWH and two-phase closed T-ET-SWH confirmed the two-phase closed T-SWH is technically more acceptable due to its higher energy efficiency with indirect fluid circulation. It presented more climate flexibility and generated more hot water per collector area compared to the single-phase T-SWH; however, it was less favorable because of the higher investment and longer cost payback period. The investment for the two-phase and single-phase T-SWHs was \$943.4 (6000 RMB) and \$833.4 (5300 RMB), respectively (Chow et al. 2013). An FPC instructed by a concrete slab consisting of metal fibers positioned in a wooden box and immersed serpentine Cu tube was economically investigated. Tests were conducted on summer and winter, and rainy days for several water flow rates. The dimples improved the temperature by 2.5 °C. The cost of a collector without a wooden box and a stand was \$97.6. The connection of the water storage tank and piping insulation was estimated at \$285.3 (Rs. 19,000), which was lower than ET-SWH (\$300.3 = Rs. 20,000). Collector cost would reduce significantly if mass procurement of materials and collector fabrication during construction of roof slab was considered (Sable 2017).

SWH integrated with the V-trough reflector could enhance the thermal performance of the SWH by the optical efficiency of about 70.5%, and the maximum temperature of 85.9 °C. The system containing the solar collector, storage tank, and pump had a fixed capital cost of \$355.9 (1489.40 RM) and a payback period of 12.2 and 8.9 years for discounted and undiscounted forms, respectively (Chong et al. 2012).

A hybrid HP-SWH was proposed to enhance the operating performance of an HP. The maximum saving was \$225.3 and \$86.5 per year compared to the electric and gas water heaters, respectively. The temperature of water increased up to 34 °C and the air source evaporator was switched to an evaporator and compensated for the ineffectiveness of the SWH at low solar radiation (Xian et al. 2020). The thermal performance of an SWH-HP with a modified solar collector was evaluated by Nuntaphan et al. (2009). The R22/R124/R152a was used as the refrigerant mixture. The COP was in the range of 2.5–5.0, and the best payback period was 2.3 years. The single solar collector produced a water temperature of 56 °C when the water tank volume was 100–300 L. A T-SWH-HP unit whose pump was powered by the steam produced by an FPC was studied by Roonprasang et al. (2008). The collector temperature was 70–90 °C, and a daily energy efficiency of 7–13% resulted. The conventional system and the proposed SWH had a price of \$1361 and \$1331 with a payback period of 9.21 and 9 years, respectively.

Challenge and prospects

Requirement for extended collecting area in FP-SWHs, a low-pressure outlet water stream in all-glass passive ET-SWHs which affects the natural circulation within tubes, decreasing the efficiency of the reflector and collectors over a long time due to being dusty or dirty (especially in PT-SWHs), higher construction and maintenance cost of ET-SWHs and PT-SWHs, heat loss from the tubes and storage tank to the environment, and the possibility of breaking the glass in all types of SWHs are the challenging issues of SWHs. The cylindrical and parabolic through types of solar water heaters rectify the requirement for a high collecting area in FPC configuration. The difficulty in the natural circulation of water within the tubes caused by the reduction in the pressure of the outlet water stream was resolved by the modification of all-glass passive circulation to all-glass active circulation and heat pipe integration to the ET-SWH arrangement. Specifically, it can be recommended that:

- The collector's orientation is required to be equipped with a sun tracker for all types of SWHs to absorb the maximum solar energy during the day.
- Evacuated tubes can be combined with CPC, creating a new design of collectors, which might be at temperatures ranging from 100 to 180 °C. This innovative type can be used to heat the high flow rates of water or produce hot water for industries (e.g., desalination processes).
- Double and triple vacuum glazing can be developed to control heat loss, which might be interesting for water heating above 120 °C.
- Replacing the glass cover of an FPC and tubes of the ETC and PTC with transparent polymers can overcome the danger of glass breaking in SWHs.
- Self-cleaning reflectors and absorbers should be developed to maximize the absorbed thermal energy over time and in dusty weather.
- Using the insulated cover during the night and baffle plate structure, PCM materials, and reverse thermosyphon valve can be some of the strategies to minimize the heat losses from the ICS-SWHs during the night.

The main objective of developments in the SWHs' design is an increase in solar collecting area and heat storage durability. Researchers can fulfill these objectives and achieve either effective designs or proper materials. The heat transfer fluid with high heat capacity using nanocomposites, application of polymeric or thermochemical materials, and PCMs can be the best options for enhancement in convective heat transfer rate, heat absorption, and

heat storage. Therefore, the main research topics arise in the field of materials research. Anti-corrosive and anti-reflective insulators, vacuum insulation, selective absorbers with long-term stability and without deterioration resulting from UV exposure, and coating of absorbers to resist stagnation temperatures should be considered in the design of SWHs.

It should be noted that a storage system based on chemical reaction has negligible losses, whereas sensible heat storage dissipates the stored thermal energy to the environment and needs to be insulated. Thermal energy storage via a controllable chemical reaction can produce higher energy compared to energy storage based on latent or sensible heat. This technique is not currently commercially viable.

Conclusions

Unique features and advantages of SWHs have turned them into attractive options for solar applications and drawn significant attention in recent years. In this work, flat plate- and concentrate-type solar collectors, ICS systems, SWHs combined with PV/T modules, solar-assisted heat pump SWHs, and SWHs using PCMs were studied based on their thermal performance, cost, energy and exergy efficiencies. The concluding remarks obtained from this review are summarized as follows:

- The performance of the SWHs is significantly changed by inlet water flow rate, the shape and number of collectors (solar collecting area), tilt angle, absorber shape, selective coating type, the existence of turbulator and agitator, using working fluid (single nanofluid and hybrid nanofluids) and PCM, incorporating storage tank, and insulator property. Optimization of operating conditions increases the convective heat transfer, thermal conductivity, Reynolds and Nusselt numbers, heat conduction rate, energy, and exergy efficiencies.
- The conventional FP-SWHs can produce hot water of about 50 °C. Using proper working fluid or electrodeposited reflector coating, CuO/H₂O nanofluids, and corrugated absorber surface produced hot water of 58–96 °C. The energy efficiency range from 63 to 86% in the modified SWHs.
- The use of ETCs led to a higher temperature (more than 80 °C) and a lower energy efficiency (less than 70%) compared to the collectors with a plane surface. ET-SWH has the disadvantages of slow water temperature increase, slow response to loading, and weak circulation of water at the lower end of the tube, but the use of HPI, turbulator, and wavy diffuse reflector overcame these problems. Using a PCM in ET-SWH for more energy storage and better heat transfer provides a satisfactory performance

over the conventional ET-SWHs. Modification of all-glass passive circulation to all-glass active circulation and heat pipe integration to the ET-SWH arrangement could rectify the difficulty in the natural circulation of water within the tubes caused by a reduction in the pressure of the outlet water stream.

- The CPC-WH type is superior to the other SWHs, particularly in achieving higher water temperatures. Using a mirror concentrator has a better performance compared to steel- and aluminum-type concentrators. The rotating mirror had about 15% higher energy efficiency in comparison with a regular mirror.
- The concentrating type of ICS-SWHs has better thermal efficiency at a reduced cost, but suffers from higher thermal losses during the night which can be resolved by using PCM.
- The SWHs containing PCM and HP with exergy efficiencies of 16% and 45% and energy efficiency of about 76% strengthened the application of these hybrid technologies.
- Economical views confirmed that the FP-SWHs have minimum production costs in the range of \$97.6–\$155.1 with a minimum payback of about 2.9 years. The linear Fresnel reflector by \$378.87 and T-ET-SWH with \$833.4 has the next ranking. The SWH-HP systems act better than electric, gas, and conventional SWHs by a cost of \$225.3, \$86.5, and \$30, respectively.
- The main objective of developments in the SWHs' design is an increase in solar collecting area and heat storage durability. Researchers can fulfill these objectives by either effective designs (using concentrating collectors) or proper materials (using nanocomposites, application of polymeric or thermochemical materials, and PCMs).

Author contributions All authors have equally contributed to the implementation of the research, to the analysis of the results, and to the writing and editing of the manuscript.

Funding Open Access funding enabled and organized by CAUL and its Member Institutions. The authors have not disclosed any funding.

Data availability Enquiries about data availability should be directed to the authors.

Declarations

Conflict of interest The authors declare that they have no known competing financial interests or personal relationships that could have appeared to influence the work reported in this paper.

Open Access This article is licensed under a Creative Commons Attribution 4.0 International License, which permits use, sharing, adaptation, distribution and reproduction in any medium or format, as long as you give appropriate credit to the original author(s) and the source,

provide a link to the Creative Commons licence, and indicate if changes were made. The images or other third party material in this article are included in the article's Creative Commons licence, unless indicated otherwise in a credit line to the material. If material is not included in the article's Creative Commons licence and your intended use is not permitted by statutory regulation or exceeds the permitted use, you will need to obtain permission directly from the copyright holder. To view a copy of this licence, visit <http://creativecommons.org/licenses/by/4.0/>.

References

- Al Imam MFI, Beg RA, Haque MJ, Rahman MS (2023) Effect of novel phase change material (PCM) encapsulated design on thermal performance of solar collector. *Result Mater*. <https://doi.org/10.1016/j.rinma.2023.100388>
- Al-Joboory HNS (2019) Comparative experimental investigation of two evacuated tube solar water heaters of different configurations for domestic application of Baghdad-Iraq. *Energy Build* 203:109437. <https://doi.org/10.1016/j.enbuild.2019.109437>
- Al-Kayiem HH, Lin SC (2014) Performance evaluation of a solar water heater integrated with a PCM nanocomposite TES at various inclinations. *Sol Energy* 109:82–92. <https://doi.org/10.1016/j.solener.2014.08.021>
- Allouhi A, Msaad AA, Amine MB, Saidur R, Mahdoui M, Kousksou T, Pandey AK, Jamil A, Moujibi N, Benbassou A (2018) Optimization of melting and solidification processes of PCM: application to integrated collector storage solar water heaters (ICSSWH). *Sol Energy* 171:562–570. <https://doi.org/10.1016/j.solener.2018.06.096>
- Al-Madani H (2006) The performance of a cylindrical solar water heater. *Renew Energy* 31:1751–1763. <https://doi.org/10.1016/j.renene.2005.09.01>
- Almeshaal M, Arunprasad V, Palaniappan M, Kolsi L (2020) Experimental study of a solar water heater fitted with spacer at the leading edge of left-right screw tapes. *Case Stud Therm Eng* 22:100777. <https://doi.org/10.1016/j.csit.2020.100777>
- Almutairi K, Mostafaeipour A, Baghaei N, Techato K, Chowdhury S, Jahangiri M, Rezaei M, Hosseini Dehshiri SJ, Goudarzi H, Issakhov A (2021) Techno-economic investigation of using solar energy for heating swimming pools in buildings and producing hydrogen: a case study. *Front Energy Res* 9:680103. <https://doi.org/10.3389/fenrg.2021.680103>
- Arab M, Abbas A (2013) Model-based design and analysis of heat pipe working fluid for optimal performance in a concentric evacuated tube solar water heater. *Sol Energy* 94:162–176. <https://doi.org/10.1016/j.solener.2013.03.029>
- Arab M, Soltanieh M, Shafii MB (2012) Experimental investigation of extra-long pulsating heat pipe application in solar water heaters. *Exp Therm Fluid Sci* 42:6–15. <https://doi.org/10.1016/j.expthermflusci.2012.03.006>
- Arun M, Barik D, Sridhar KP, Vignesh G (2020) Experimental and CFD analysis of plain and dimples tube at application of solar water heater. *Mater Today Proc* 2020(42):804–809. <https://doi.org/10.1016/j.matpr.2020.09.79>
- Avargani VM, Rahimi A, Divband M (2020) Coupled optical and thermal analyses of a new type of solar water heaters using parabolic trough reflectors. *Sust Energy Technol Assess* 40:100780. <https://doi.org/10.1016/j.seta.2020.100780>
- Bahrami A, Okoye CO, Pourasl HH, Khojastehnezhad VM (2022) Techno-economic comparison of fixed and tracking flat plate solar collectors in the northern hemisphere. *J Clean Prod* 378:134523. <https://doi.org/10.1016/j.jclepro.2022.134523>
- Bazri S, Badruddin IA, Naghavi MS, Seng OK, Wongwises S (2019) An analytical and comparative study of the charging and

- discharging processes in a latent heat thermal storage tank for solar water heater system. *Sol Energy* 185:424–438. <https://doi.org/10.1016/j.solener.2019.04.046>
- Bello M, Shanmugan S (2020) Achievements in mid and high-temperature selective absorber coatings by physical vapor deposition (PVD) for solar thermal application-A review. *J Alloys Compd* 839:155510. <https://doi.org/10.1016/j.jallco.2019.155510>
- Benrejeb R, Helal O, Chaouachi B (2016) Study of the effect of truncation on the optical and thermal performances of an ICS solar water heater system. *Sol Energy* 132:84–95. <https://doi.org/10.1016/j.solener.2016.02.057>
- Bhakta AK, Panday NK, Singh SN (2018) Performance study of a cylindrical parabolic concentrating solar water heater with nail type twisted tape inserts in the copper absorber tube. *Energies* 11:204. <https://doi.org/10.3390/en11020204>
- Bouhal T, Agrouaz Y, Allouhi A, Kousksou T, Jamil A, El Rhafiki T, Zeraoui Y (2017) Impact of load profile and collector technology on the fractional savings of solar domestic water heaters under various climatic conditions. *Int J Hydrog Energy* 42:13245–13258. <https://doi.org/10.1016/j.ijhydene.2017.03.226>
- Bouhal T, El Rhafiki T, Kousksou T, Jamil A, Zeraoui Y (2018) PCM addition inside solar water heaters: Numerical comparative approach. *J Energy Storage* 19:232–246. <https://doi.org/10.1016/j.est.2018.08.005>
- Bracamonte J (2017) Effect of the transient energy input on thermodynamic performance of passive water-in-glass evacuated tube solar water heaters. *Renew Energy* 105:689–701. <https://doi.org/10.1016/j.renene.2016.12.051>
- Bracamonte J, Parada J, Dimas J, Baritto M (2015) Effect of the collector tilt angle on thermal efficiency and stratification of passive water in glass evacuated tube solar water heater. *Appl Energy* 155:648–659. <https://doi.org/10.1016/j.apenergy.2015.06.008>
- Budihardjo I, Morrison GL (2009) Performance of water-in-glass evacuated tube solar water heaters. *Sol Energy* 83:49–56. <https://doi.org/10.1016/j.solener.2008.06.010>
- Cao Y, Mihardj LW, Parikhani T (2020) Thermal performance, parametric analysis, and multi-objective optimization of a direct-expansion solar-assisted heat pump water heater using NSGA-II and decision makings. *Appl Therm Eng* 181:115892. <https://doi.org/10.1016/j.applthermaleng.2020.115892>
- Ceylan I (2012) Energy and exergy analyses of a temperature controlled solar water heater. *Energy Build* 47:630–635. <https://doi.org/10.1016/j.enbuild.2011.12.040>
- Chaabane M, Mhiri H, Bournot P (2014) Thermal performance of an integrated collector storage solar water heater (ICSSWH) with phase change materials (PCM). *Energy Convers Manag* 78:897–903. <https://doi.org/10.1016/j.enconman.2013.07.089>
- Chargui R, Tashtoush B (2021) Thermoeconomic analysis of solar water heaters integrating phase change material modules and mounted in football pitches in tunisia. *J Energy Stor* 33:102129. <https://doi.org/10.1016/j.est.2020.102129>
- Chen J, Yu J (2018) Energy and exergy analysis of a new direct-expansion solar assisted vapor injection heat pump cycle with subcooler for water heater. *Sol Energy* 171:613–620. <https://doi.org/10.1016/j.solener.2018.07.019>
- Chong KK, Chay KG, Chin KH (2012) Study of a solar water heater using stationary V-trough collector. *Renew Energy* 39:207–215. <https://doi.org/10.1016/j.renene.2011.08.002>
- Chow TT, Bai Y, Dong Z, Fong KF (2013) Selection between single-phase and two-phase evacuated-tube solar water heaters in different climate zones of China. *Sol Energy* 98:265–274. <https://doi.org/10.1016/j.solener.2013.10.011>
- Curry C, Cherni JA, Mapako M (2017) The potential and reality of the solar water heater programme in South African townships: lessons from the city of Tshwane. *Energy Policy* 106:75–84. <https://doi.org/10.1016/j.enpol.2017.03.028>
- Darbari B, Rashidi S (2021) Thermal efficiency of flat plate thermosyphon solar water heater with nanofluids. *J Taiwan Inst Chem Eng* 128:276–287. <https://doi.org/10.1016/j.jtice.2021.06.027>
- Deng W, Yu J (2016) Simulation analysis on dynamic performance of a combined solar/air dual source heat pump water heater. *Energy Convers Manag* 120:378–387. <https://doi.org/10.1016/j.enconman.2016.04.102>
- Dharuman C, Arakeri JH, Srinivasan K (2006) Performance evaluation of an integrated solar water heater as an option for building energy conservation. *Energy Build* 38:214–219. <https://doi.org/10.1016/j.enbuild.2005.05.007>
- Dhinakaran R, Muraliraja R, Elansezhian R, Baskar S, Satish S, Shaisundaram VS (2020) Utilization of solar resource using phase change material assisted solar water heater and the influence of nano filler. *Mater Today Proceed* 37:1281–1285. <https://doi.org/10.1016/j.matpr.2020.06>
- Duarte WM, Rabelo SN, Paulino TF, Pabón JJ, Machado L (2021) Experimental performance analysis of a CO₂ direct-expansion solar assisted heat pump water heater. *Int J Refrig* 125:52–63. <https://doi.org/10.1016/j.ijrefrig.2021.01.008>
- Edwin M, Eniyan MC, Percy AJ (2023) Spiral tube solar water heating computational analysis with concrete absorber: A CFD approach. *Mater Today Proceed*. <https://doi.org/10.1016/j.matpr.2023.02.307>
- Eskin N (2000) Performance analysis of a solar process heat system. *Energy Convers Manag* 41:1141–1154. [https://doi.org/10.1016/S0196-8904\(99\)00165-X](https://doi.org/10.1016/S0196-8904(99)00165-X)
- Faddouli A, Fadili S, Labrim H, Hartiti B, Ertugrul M, Belouggadia N, Stitou M (2020) Comparative study of a normal solar water heater and smart thermal/thermoelectric hybrid systems. *Mater Today Proceed* 30:1039–1042. <https://doi.org/10.1016/j.matpr.2020.04.499>
- Farzan H, Ameri M, Mahmoudi M (2023) Thermal assessment of a new planar thermal diode integrated collector storage solar water heater in different partial vacuums: an experimental study. *Renew Energy* 208:119–129. <https://doi.org/10.1016/j.renene.2023.03.071>
- Gertzos KP, Pnevmatikakis SE, Caouris YG (2008) Experimental and numerical study of heat transfer phenomena, inside a flat-plate integrated collector storage solar water heater (ICSSWH), with indirect heat withdrawal. *Energy Convers Manag* 49:3104–3115. <https://doi.org/10.1016/j.enconman.2008.06.005>
- Gilani HA, Hoseinzadeh S (2021) Techno-economic study of compound parabolic collector in solar water heating system in the northern hemisphere. *Appl Therm Eng* 190:116756. <https://doi.org/10.1016/j.applthermaleng.2021.116756>
- Gunasekaran N, Kumar PM, Raja S, Sharavanan S, Avinas K, Kannan PA, Gokul S (2021) Investigation on ETC solar water heater using twisted tape inserts. *Mater Today Proceed* 47:5011–5016. <https://doi.org/10.1016/j.matpr.2021.04.586>
- Hajabdollahi Z, Hajabdollahi H (2017) Thermo-economic modeling and multi-objective optimization of solar water heater using flat plate collectors. *Sol Energy* 155:191–202. <https://doi.org/10.1016/j.solener.2017.06.023>
- Hamed M, Fallah A, Brahim AB (2017) Numerical analysis of charging and discharging performance of an integrated collector storage solar water heater. *Int J Hydrog Energy* 42:8777–8789. <https://doi.org/10.1016/j.ijhydene.2016.11.179>
- Harmim A, Boukar M, Amar M, Haida A (2019) Simulation and experimentation of an integrated collector storage solar water heater designed for integration into building facade. *Energy* 166:59–71. <https://doi.org/10.1016/j.energy.2018.10.069>
- Ho CD, Chen TC, Tsai CJ (2010) Experimental and theoretical studies of recyclic flat-plate solar water heaters equipped with rectangle

- conduits. *Renew Energy* 35:2279–2287. <https://doi.org/10.1016/j.renene.2010.03.026>
- Hossain MS, Saidur R, Fayaz H, Rahim NA, Islam MR, Ahamed JU, Rahman MM (2011) Review on solar water heater collector and thermal energy performance of circulating pipe. *Renew Sust Energy Rev* 15:3801–3812. <https://doi.org/10.1016/j.rser.2011.06.008>
- Hussain MI, Lee GH (2014) Thermal performance evaluation of a conical solar water heater integrated with a thermal storage system. *Energy Convers Manag* 87:267–273. <https://doi.org/10.1016/j.enconman.2014.07.023>
- Isravel RS, Raja M, Saravanan S, Vijayan V (2020) Thermal augmentation in parabolic trough collector solar water heater using rings attached twisted tapes. *Mater Today Proceed* 21:127–129. <https://doi.org/10.1016/j.matpr.2019.05.375>
- Izgi B, Arslan M (2022) Effect of phase change material on thermal stratification of solar hot water tank with a mantle: a numerical analysis. *J Energy Stor* 52:105078. <https://doi.org/10.1016/j.est.2022.105078>
- Janardhana K, Sivakumar A, Gladson GJN, Ramesh C, Musthafa AS, Gopinathan R (2022) Study on the performance of a flat plate solar water heater using a hybrid nanofluid. *Mater Today Proceed* 69:1145–1149. <https://doi.org/10.1016/j.matpr.2022.08.181>
- Jing OL, Bashir MJ, Kao JJ (2015) Solar radiation based benefit and cost evaluation for solar water heater expansion in Malaysia. *Renew Sust Energy Rev* 48:328–335. <https://doi.org/10.1016/j.rser.2015.04.031>
- Kanimozhi B, Bedford SP, Kanth KS, Kumar SV (2019) Experimental analysis of solar water heater using porous medium with agitator. *Mater Today Proceed* 16:1204–1211. <https://doi.org/10.1016/j.matpr.2019.05.215>
- Karwa R, Sharma C (2018) Performance study of once-through solar water heater. *IOSR J Mech Civil Eng* 15:46–65. <https://doi.org/10.9790/1684-1502054665>
- Kee SY, Munusamy Y, Ong KS (2018) Review of solar water heaters incorporating solid-liquid organic phase change materials as thermal storage. *Appl Therm Eng* 131:455–471. <https://doi.org/10.1016/j.applthermaleng.2017.12.032>
- Koffi PME, Koua BK, Gbaha P, Touré S (2014) Thermal performance of a solar water heater with internal exchanger using thermosiphon system in Côte d'Ivoire. *Energy* 64:187–199. <https://doi.org/10.1016/j.energy.2013.09.059>
- Kong X, Jiang K, Dong S, Li Y, Li J (2018) Control strategy and experimental analysis of a direct-expansion solar-assisted heat pump water heater with R134a. *Energy* 145:17–24. <https://doi.org/10.1016/j.energy.2017.12.114>
- Kong X, Li J, Wang B, Li Y (2020a) Numerical study of a direct-expansion solar-assisted heat pump water heater under frosting conditions based on experiments. *Sol Energy* 196:10–21. <https://doi.org/10.1016/j.solener.2019.11.104>
- Kong X, Yang Y, Zhang M, Li Y, Li J (2020b) Experimental investigation on a direct-expansion solar-assisted heat pump water heater using R290 with micro-channel heat transfer technology during the winter period. *Int J Refrig* 113:38–48. <https://doi.org/10.1016/j.ijrefrig.2020.01.019>
- Kong X, Zhang M, Yang Y, Li Y, Wang D (2020c) Comparative experimental analysis of direct-expansion solar-assisted heat pump water heaters using R134a and R290. *Sol Energy* 203:187–196. <https://doi.org/10.1016/j.solener.2020.04.048>
- Kong X, Wang B, Shang Y, Li J, Li Y (2020) Influence of different regulation modes of compressor speed on the performance of direct-expansion solar-assisted heat pump water heater. *Appl Therm Eng* 169:115007
- Koroneos CJ, Nanaki EA (2012) Life cycle environmental impact assessment of a solar water heater. *J Clean Prod* 37:154–161. <https://doi.org/10.1016/j.jclepro.2012.07.001>
- Ktistis PK, Agathokleous RA, Kalogirou SA (2021) Experimental performance of a parabolic trough collector system for an industrial process heat application. *Energy* 215:119288. <https://doi.org/10.1016/j.energy.2020.119288>
- Kumar PM, Mysamy K (2020) A comprehensive study on thermal storage characteristics of nano-CeO₂ embedded phase change material and its influence on the performance of evacuated tube solar water heater. *Renew Energy* 162:662–676. <https://doi.org/10.1016/j.renene.2020.08.122>
- Kumar A, Prasad BN (2000) Investigation of twisted tape inserted solar water heaters—heat transfer, friction factor and thermal performance results. *Renew Energy* 19:379–398. [https://doi.org/10.1016/S0960-1481\(99\)00061-0](https://doi.org/10.1016/S0960-1481(99)00061-0)
- Kumar M, Negi BS, Grewal R, Manchanda H (2023) Assessment of an ETC based solar water heater at different tilt angles. *Mater Today Proceed*. <https://doi.org/10.1016/j.matpr.2023.02.263>
- Li Z, Ma L, Li Z, Ni W (2019) Multi-energy cooperative utilization business models: a case study of the solar-heat pump water heater. *Renew Sust Energy Rev* 108:392–397. <https://doi.org/10.1016/j.rser.2019.04.015>
- Li M, Bi Y, Fang J, Wei J (2022) An optical concentrator coupled multistage solar steam generation system for solar thermal-latent heat cascade utilization and water desalination: performance and economic benefit analysis. *Sep Purif Technol* 303:122191. <https://doi.org/10.1016/j.seppur.2022.122191>
- Li J, Wei S, Dong Y, Liu X, Novakovic V (2023) Technical and economic performance study on winter heating system of air source heat pump assisted solar evacuated tube water heater. *Appl Therm Eng* 221:119851. <https://doi.org/10.1016/j.applthermaleng.2022.119851>
- Lin WM, Chang KC, Chung KM (2015) Payback period for residential solar water heaters in Taiwan. *Renew Sust Energy Rev* 41:901–906. <https://doi.org/10.1016/j.rser.2014.09.005>
- Liu M, Saman W, Bruno F (2012) Review on storage materials and thermal performance enhancement techniques for high temperature phase change thermal storage systems. *Renew Sust Energy Rev* 16:2118–2132. <https://doi.org/10.1016/j.rser.2012.01.010>
- Lizama-Tzec FI, Herrera-Zamora DM, Arés-Muzio O, Gómez-Espinoza VH, Santos-González I, Cetina-Dorantes M, Vega-Poot AG, García-Valladares O, Oskam G (2019) Electrodeposition of selective coatings based on black nickel for flat-plate solar water heaters. *Sol Energy* 194:302–310. <https://doi.org/10.1016/j.solener.2019.10>
- Mamouri SJ, Bénard A (2018) New design approach and implementation of solar water heaters: a case study in Michigan. *Sol Energy* 162:165–177. <https://doi.org/10.1016/j.solener.2018.01.028>
- Mandal SK, Kumar S, Kumar Singh P, Mishra SK, Bishwakarma H, Choudhry NP, Kumar Nayak R, Kumar DA (2019) Performance investigation of CuO-paraffin wax nanocomposite in solar water heater during night. *Thermochim Acta* 671:36–42. <https://doi.org/10.1016/j.tca.2018.11.003>
- Mandal SK, Kumar S, Kumar Singh P, Kumar Mishra S, Singh DK (2020) Performance investigation of nanocomposite based solar water heater. *Energy* 198:117295. <https://doi.org/10.1016/j.energy.2020.117295>
- Manirathnam AS, Dhanush Manikandan MK, Hari Prakash R, Kamesh Kumar B, Deepan AM (2021) Experimental analysis on solar water heater integrated with nano composite phase change material (SCi and CuO). *Mater Today Proceed* 37:232–240. <https://doi.org/10.1016/j.matpr.2020.05.010>
- Milani D, Abbas A (2016) Multiscale modeling and performance analysis of evacuated tube collectors for solar water heaters using

- diffuse flat reflector. *Renew Energy* 86:360–374. <https://doi.org/10.1016/j.renene.2015.08.013>
- Mokhlif ND, Eleiwi MA, Yassen TA (2021) Experimental investigation of a double glazing integrated solar water heater with corrugated absorber surface. *Mater Today Proc* 42:2742–2748. <https://doi.org/10.1016/j.matpr.2020.12.714>
- Muhumuza R, Zacharopoulos A, Mondol JD, Smyth M, Pugsley A, Giuzio GF, Kurmis D (2019) Experimental investigation of horizontally operating thermal diode solar water heaters with differing absorber materials under simulated conditions. *Renew Energy* 138:1051–1064. <https://doi.org/10.1016/j.renene.2019.02.036>
- Nahar NM (2002) Capital cost and economic viability of thermosyphonic solar water heaters manufactured from alternate materials in India. *Renew Energy* 26:623–635. [https://doi.org/10.1016/S0960-1481\(00\)1501-1](https://doi.org/10.1016/S0960-1481(00)1501-1)
- Najafabadi MF, Farhadi M, Rostami HT (2022) Numerically analysis of a phase-change material in concentric double-pipe helical coil with turbulent flow as thermal storage unit in solar water heaters. *J Energy Stor* 55:105712. <https://doi.org/10.1016/j.est.2022.105712>
- Nasirov S, Carredano N, Agostini CA, Silva C (2021) Public perception and adoption of Solar Water Heating systems in Chile: the role of supply side income tax credits. *Renew Sustain Energy Rev* 135:110389. <https://doi.org/10.1016/j.rser.2020.110389>
- Nazari M, Jafarmadar S, Khalilarya S (2022) Exergy and thermoeconomic analyses of serpentine tube flat-plate solar water heaters coated with CuO nanostructures. *Case Stud Therm Eng* 35:102072. <https://doi.org/10.1016/j.csite.2022.102072>
- Nirmala PN (2020) Comparative studies on efficiency of single and double glassed solar water heater. *Mater Today Proceed* 34:420–424. <https://doi.org/10.1016/j.matpr.2020.02.204>
- Nuntaphan A, Chansena C, Kiatsiriroat T (2009) Performance analysis of solar water heater combined with heat pump using refrigerant mixture. *Appl Energy* 86:748–756. <https://doi.org/10.1016/j.apenergy.2008.05.014>
- Panahi R, Khanjanpour MH, Javadi A, Akrami M, Rahnama M, Ameri M (2019) Analysis of the thermal efficiency of a compound parabolic Integrated Collector Storage solar water heater in Kerman, Iran. *Sust Energy Technol Assess* 36:100564
- Pandya H, Behura AK (2017) Experimental study of V-through solar water heater for tilt angle and glass transmissivity. *Energy Procedia* 109:377–384. <https://doi.org/10.1016/j.egypro.2017.03.034>
- Papadimitratos A, Sobhansarbandi S, Pozdin V, Zakhidov A, Hassanipour F (2016) Evacuated tube solar collectors integrated with phase change materials. *Sol Energy* 129:10–19. <https://doi.org/10.1016/j.solener.2015.12.040>
- Patel K, Patel P, Patel J (2012) Review of solar water heating systems. *Int J Adv Eng Technol* 3:146–149
- Pathak A, Bhosle A, Baste P, Kurhe N, Suryawanshi N, Marathe A, Jadkar S (2021) Performance comparison of CPC based solar installations at different locations in India and analysis of variation pattern. In: *IOP Conference Series: Earth and Environmental Science*, vol 850. IOP Publishing, pp 012039. <https://doi.org/10.1088/1755-1315/850/1/012039>
- Peng L, Salem M, Blazek V, Prokop L, Al-Bahrani M, Misak S (2023) Thermal energy storage applications in solar water heaters: an updated review. *Sustain Energy Technol Assess* 57:103230. <https://doi.org/10.1016/j.seta.2023.103230>
- Rahimi-Ahar Z, Hatamipour MS (2020) A perspective of thermal type desalination: technology, current development and thermodynamics analysis. *Encyclopedia of Life Support Systems (EOLSS)* 2020. <http://www.eolss.net/Eolss-sampleAllChapter.aspx>
- Rahimi-Ahar Z, Hatamipour MS, Ghalavand Y, Palizvan A (2020) Comprehensive study on vacuum humidification-dehumidification (VVDH) desalination. *Appl Therm Eng* 169:114944. <https://doi.org/10.1016/j.applthermaleng.2020.114944>
- Rahimi-Ahar Z, Hatamipour MS (2023) Exergy analysis of thermal desalination processes: a review. *Clean Technol Environ Policy* 3:1–28. <https://doi.org/10.1007/s10098-023-02491-6>
- Ram kumar R, Suthahar SJ, Sakthivel C, Vijayan V, Yokeshwaran R (2020) Performance analysis of solar water heater by using TiO₂ nanofluids. *Mater Today Proceed* 21:817–819. <https://doi.org/10.1016/j.matpr.2019.07.251>
- Ramesh C, Vijayakumar M, Alshahrani S, Navaneethakrishnan G, Palanisamy R, Natrayan L, Saleel CA, Afzal A, Shaik S, Panchal H (2022) Performance enhancement of selective layer coated on solar absorber panel with reflector for water heater by response surface method: a case study. *Case Stud Therm Eng* 36:102093. <https://doi.org/10.1016/j.csite.2022.102093>
- Rao YA, Somwanshi A (2022) A comprehensive review on integrated collector-storage solar water heaters. *Mater Today Proc*. <https://doi.org/10.1016/j.matpr.2021.12.424>
- Redpath DA (2012) Thermosyphon heat-pipe evacuated tube solar water heaters for northern maritime climates. *Sol Energy* 86:705–715. <https://doi.org/10.1016/j.solener.2011.11.015>
- Rezvani S, Bahri PA, Urmee T, Baverstock GF, Moore AD (2017) Techno-economic and reliability assessment of solar water heaters in Australia based on Monte Carlo analysis. *Renew Energy* 105:774–785. <https://doi.org/10.1016/j.renene.2017.01.005>
- Roberts DE (2013) A figure of merit for selective absorbers in flat plate solar water heaters. *Sol Energy* 98:503–510. <https://doi.org/10.1016/j.solener.2013.10.012>
- Robles A, Duong V, Martin AJ, Guadarrama JL, Diaz G (2014) Aluminum minichannel solar water heater performance under year-round weather conditions. *Sol Energy* 110:356–364. <https://doi.org/10.1016/j.solener.2014.09.031>
- Rohit Khargotra RK, Kumar S (2021) Influence of hindrance promoter on the thermal augmentation factor of solar water heater (an experimental study). *Renew Energy* 163:1356–1369. <https://doi.org/10.1016/j.renene.2020.0>
- Roonprasang N, Namprakai P, Pratinthong N (2008) Experimental studies of a new solar water heater system using a solar water pump. *Energy* 33:639–646. <https://doi.org/10.1016/j.energy.2007.12.002>
- Sable A (2017) Experimental and economic analysis of concrete absorber collector solar water heater with use of dimpled tube. *Resource-Efficient Technol* 3:483–490. <https://doi.org/10.1016/j.refit.2017.06.001>
- Sadeghi G, Safarzadeh H, Bahiraei M, Ameri M, Raziani M (2019) Comparative study of air and argon gases between cover and absorber coil in a cylindrical solar water heater: an experimental study. *Renew Energy* 135:426–436. <https://doi.org/10.1016/j.renene.2018.12.0>
- Sadeghi G, Mehrali M, Shahi M, Brem G (2022) Experimental analysis of shape-stabilized PCM applied to a direct-absorption evacuated tube solar collector exploiting sodium acetate trihydrate and graphite. *Energy Convers Manag* 269:116176. <https://doi.org/10.1016/j.enconman.2022.116176>
- Sae-Jung P, Krittanawach T, Deedom P, Limmeechokchai B (2015) An experimental study of thermo-syphon solar water heater in thailand. *Energy Procedia* 79:442–447. <https://doi.org/10.1016/j.egypro.2015.11.516>
- Said Z, Ghodbane M, Tiwari AK, Ali HM, Boumeddane B, Ali ZM (2021) 4E (energy, exergy, economic, and environment) examination of a small LFR solar water heater: An experimental and numerical study. *Case Stud Therm Eng* 27:101277. <https://doi.org/10.1016/j.csite.2021.101277>
- Saravanan A, Senthilkumaar JS, Jaisankar S (2016) Performance assessment in V-trough solar water heater fitted with square

- and V-cut twisted tape inserts. *Appl Therm Eng* 102:476–486. <https://doi.org/10.1016/j.applthermaleng.2016.0>
- Sari A, Kaygusuz K (2001) Thermal energy storage system using stearic acid as a phase change material. *Sol Energy* 71:365–376. [https://doi.org/10.1016/S0038-092X\(01\)00075-5](https://doi.org/10.1016/S0038-092X(01)00075-5)
- Shafieian A, Khiadani M, Nosrati A (2019a) Thermal performance of an evacuated tube heat pipe solar water heating system in cold season. *Appl Therm Eng* 149:644–657. <https://doi.org/10.1016/j.applthermaleng.2018.12.078>
- Shafieian A, Osman JJ, Khiadani M, Nosrati A (2019b) Enhancing heat pipe solar water heating systems performance using a novel variable mass flow rate technique and different solar working fluids. *Sol Energy* 186:191–203. <https://doi.org/10.1016/j.solener.2019.05.016>
- Shalaby SM, Kabeel AE, Moharram BM, Fleafl AH (2020) Experimental study of the solar water heater integrated with shell and finned tube latent heat storage system. *J Energy Storage* 31:101628. <https://doi.org/10.1016/j.est.2020.101628>
- Sharma N (2021) Public perceptions towards adoption of residential solar water heaters in USA: a case study of Phoenixians in Arizona. *J Clean Prod* 320:128891. <https://doi.org/10.1016/j.jclepro.2021.128891>
- Sharma MK (2022) Alternative designs and technological advancements of phase change material integrated photovoltaics: a state-of-the-art review. *J Energy Stor* 48:104020. <https://doi.org/10.1016/j.est.2022.104020>
- Shrivastava RL, Kumar V, Untawale SP (2017) Modeling and simulation of solar water heater: a TRNSYS perspective. *Renew Sust Energ Rev* 67:126–143. <https://doi.org/10.1016/j.rser.2016.09.005>
- Siampour L, Vahdatpour S, Jahangiri M, Mostafaeipour A, Goli A, Alidadi Shamsabadi A (2021) Techno-enviro assessment and ranking of Turkey for use of home-scale solar water heaters. *Sustain Energy Technol Assess* 43:100948. <https://doi.org/10.1016/j.seta.2020.100948>
- Da Silva FA, Dezan DJ, Pantaleao AV, Salviano LO (2019) Longitudinal vortex generator applied to heat transfer enhancement of a flat plate solar water heater. *Appl Therm Eng* 158:113790. <https://doi.org/10.1016/j.appltherma>
- Siritan M, Kammuang-Lue N, Terdtoon P, Sakulchangsattajai P (2022) Thermal performance and thermo-economics analysis of evacuated glass tube solar water heater with closed-loop pulsating heat pipe. *Case Stud Therm Eng* 35:102139. <https://doi.org/10.1016/j.csite.2022.102139>
- Sivasubramanian R, Kumaresan G, Santhosh N, Reshvanth KS, Riyasudeen SS, Medone RS (2022) Performance analysis of multipass tubes solar water heater using nanofluids. *Mater Today Proceed* 66:1051–1055. <https://doi.org/10.1016/j.matpr.2022.04.838>
- Smyth M, Eames PC, Norton B (2004) Techno-economic appraisal of an integrated collector/storage solar water heater. *Renew Energy* 29:1503–1514. <https://doi.org/10.1016/j.renene.2003.10.009>
- Smyth M, McGarrigle P, Eames PC, Norton B (2005) Experimental comparison of alternative convection suppression arrangements for concentrating integral collector storage solar water heaters. *Sol Energy* 78:223–233. <https://doi.org/10.1016/j.solener.2004.06.004>
- Strielkowski W, Civiń L, Tarkhanova E, Tvaronavičienė M, Petrenko Y (2021) Renewable energy in the sustainable development of electrical power sector: a review. *Energies* 14:8240. <https://doi.org/10.3390/en14248240>
- Taheri Y, Ziapour BM, Alimardani K (2013) Study of an efficient compact solar water heater. *Energy Convers Manag* 70:187–193. <https://doi.org/10.1016/j.enconman.2013.02.014>
- Taherian H, Rezanian A, Sadeghi S, Ganji DD (2011) Experimental validation of dynamic simulation of the flat plate collector in a closed thermosyphon solar water heater. *Energy Convers Manag* 52:301–307. <https://doi.org/10.1016/j.enconman.2010.06.063>
- Tamuli BR, Nath S (2023) Analysis of micro heat pipe array based evacuated tube solar water heater integrated with an energy storage system for improved thermal performance. *Therm Sci Eng Prog* 41:101801. <https://doi.org/10.1016/j.tsep.2023.101801>
- Tanha K, Fung AS, Kumar R (2015) Performance of two domestic solar water heaters with drain water heat recovery units: Simulation and experimental investigation. *Appl Therm Eng* 90:444–459. <https://doi.org/10.1016/j.applthermaleng.2015.07.038>
- Tarhan S, Sari A, Yardim MH (2006) Temperature distributions in trapezoidal built in storage solar water heaters with/without phase change materials. *Energy Convers Manag* 47:2143–2154. <https://doi.org/10.1016/j.enconman.2005>
- Thangavelu SK, Khoo RJ, Piraiarasi C (2021) Exergy and exergoeconomic analysis of domestic scale solar water heater by the effect of solar collector. *Mater Today Proc* 47:5004–5010. <https://doi.org/10.1016/j.matpr.2021.04.584>
- Touaba O, Oussama Ait Cheikh MS, El-Amine Slimani M, Bouraiou A, Ziane A, Necaibia A, Harmim A (2020) Experimental investigation of solar water heater equipped with a solar collector using waste oil as absorber and working fluid. *Sol Energy* 199:630–644. <https://doi.org/10.1016/j.solener.2020.02>
- Uctug FG, Azapagic A (2018) Life cycle environmental impacts of domestic solar water heaters in Turkey: the effect of different climatic regions. *Sci Total Environ* 622:1202–1216. <https://doi.org/10.1016/j.scitotenv.2017.12.057>
- Vasanthaseelan S, Kumar PM, Anandkumar R, Ram KH, Subbiah R, Suresh V, Balaji SV (2021) Investigation on solar water heater with different types of turbulators. *Mater Today Proceed* 47:5203–5208. <https://doi.org/10.1016/j.matpr.2021>
- Vengadesan E, Senthil R (2020) A review on recent development of thermal performance enhancement methods of flat plate solar water heater. *Sol Energy* 206:935–961. <https://doi.org/10.1016/j.solener.2020.06>
- Wannagosit C, Sakulchangsattajai P, Kammuang-Lue N, Terdtoon P (2018) Validated mathematical models of a solar water heater system with thermosyphon evacuated tube collectors. *Case Stud Therm Eng* 12:528–536. <https://doi.org/10.1016/j.csite.2018.07.005>
- Xian T, Wu J, Zhang, X (2020) Study on the operating characteristics of a solar heat pump water heater based on data fusion. *Sol Energy* 212:113–124. <https://doi.org/10.1016/j.solener.2020.10>
- Xie B, Li C, Zhang B, Yang L, Guiyu Xiao JC (2020) Evaluation of stearic acid/coconut shell charcoal composite phase change thermal energy storage materials for tankless solar water heater. *Energy Built Environ* 1:187–198. <https://doi.org/10.1016/j.enbenv.2019.08.0>
- Xue HS (2016) Experimental investigation of a domestic solar water heater with solar collector coupled phase-change energy storage. *Renew Energy* 86:257–261. <https://doi.org/10.1016/j.renene.2015.08.017>
- Yamaguchi Y, Akai K, Shen J, Fujimura N, Shimoda Y, Saijo T (2013) Prediction of photovoltaic and solar water heater diffusion and evaluation of promotion policies on the basis of consumers' choices. *Appl Energy* 102:1148–1159. <https://doi.org/10.1016/j.apenergy.2012.06.037>
- Yari S, Safarzadeh H, Bahiraei M (2023) Experimental study of storage system of a solar water heater equipped with an innovative absorber spherical double-walled tank immersed in a phase change material. *J Energy Stor* 61:106782. <https://doi.org/10.1016/j.est.2023.106782>
- Yassen TA, Mokhlif ND, Eleiwi MA (2019) Performance investigation of an integrated solar water heater with corrugated absorber surface for domestic use. *Renew Energy* 138:852–860. <https://doi.org/10.1016/j.renene.2019.01.114>

- Yehualashet KN, Fatoba O, Asfaw SM (2022) Experimental study and numerical analysis of thermal performance of corrugated plate solar collector. *Mater Today Proceed* 62:2849–2856. <https://doi.org/10.1016/j.matpr.2022.02.414>
- Yılmaz İH, Söylemez MS, Yumrutaş R (2023) Experimental analysis and dynamic simulation of a solar-assisted industrial process using parabolic trough solar collectors under outdoor conditions. *Energy Sust Develop* 72:212–229. <https://doi.org/10.1016/j.esd.2022.12.017>
- Yu Z, Huang P (2020) Local governments' incentives and governing practices in low-carbon transition: A comparative study of solar water heater governance in four Chinese cities. *Cities* 96:102477. <https://doi.org/10.1016/j.cities.2019.102477>
- Ziapour BM, Aghamiri A (2014) Simulation of an enhanced integrated collector–storage solar water heater. *Energy Convers Manag* 78:193–203. <https://doi.org/10.1016/j.enconman.2013.10.068>
- Ziapour BM, Khalili MB (2016) PVT type of the two-phase loop mini tube thermosyphon solar water heater. *Energy Convers Manag* 129:54–61. <https://doi.org/10.1016/j.enconman.2016.10.004>

Publisher's Note Springer Nature remains neutral with regard to jurisdictional claims in published maps and institutional affiliations.